

Pion Electroproduction Amplitude Relations in the $1/N_c$ Expansion

Richard F. Lebed* and Lang Yu†

Department of Physics, Arizona State University, Tempe, AZ 85287-1504

(Dated: April 2009)

Abstract

We derive expressions for pion electroproduction amplitudes in the $1/N_c$ expansion of QCD, and obtain from them linear relations between the electromagnetic multipole amplitudes that hold at all energies. The leading-order relations in $1/N_c$ compare favorably with available data (especially away from resonances), but the next-to-leading-order relations tend to provide only small or no improvement.

PACS numbers: 11.15.Pg, 13.60.Le, 25.30.Rw

arXiv:0905.0122v2 [hep-ph] 12 Oct 2009

*Electronic address: Richard.Lebed@asu.edu

†Electronic address: langyu@asu.edu

I. INTRODUCTION

The $1/N_c$ expansion of QCD [1], where N_c is the number of color charges, has emerged as one of the principal tools for studying low-energy hadronic processes and hadron static observables. In the simplest construction, baryons are assembled from a collection of N_c quarks, each one transforming under the $SU(N_c)$ fundamental representation, such that the aggregate forms a color singlet [2]. While analyzing baryons using the N_c quarks' spin-flavor and combinatoric properties has led to a large variety of interesting results far too numerous to review here [3], the most compelling physical picture for describing the dynamical properties of large N_c baryons (particularly scattering amplitudes) is the chiral soliton approach [4] originally motivated by the Skyrme model [5]. One of the most intriguing properties of these studies is the emergence of model-independent linear relations among meson-baryon scattering amplitudes [6], whose origin gradually became understood as connected to the large N_c limit [7, 8]. In fact, the existence of such relations can be traced back to the contracted $SU(4)$ spin-flavor symmetry that emerges in the single-baryon sector as $N_c \rightarrow \infty$, which in turn is obtained by demanding consistent order-by-order unitarity in meson-baryon scattering processes [9, 10, 11]; the fact that the former can be derived from the latter was first demonstrated in Refs. [12].

The large N_c scattering method [12] explains the existence of baryon resonance multiplets that share similarities (but are not identical to) those appearing in large N_c quark models; in particular, one can study resonances with arbitrarily large widths [13], exotics [14], and three-flavor resonances [15]. In addition, the means by which the spurious $N_c > 3$ states may be removed [16] has been explored, as well as the nature of the competing chiral and large N_c limits [17], and results for multipion processes [18].

An essential ingredient to obtaining results useful for $N_c = 3$ phenomenology is understanding how to include $1/N_c$ corrections. The original large N_c scattering amplitude relations were noted long ago to satisfy the t -channel isospin-spin exchange constraint $I_t = J_t$ [8]. Using operator techniques, Ref. [19] showed that static pion-baryon couplings with $I \neq J$ are suppressed by a relative factor of $1/N_c^{|I-J|}$, and the same techniques were used to show [20] that nucleon-nucleon interactions with $|I_t - J_t| = n$ are suppressed by $1/N_c^n$. Much more recently, the same techniques were used to show [21] the analogous result for t -channel pion-baryon scattering amplitudes. The expression of these pion-baryon constraints in terms of

s -channel observables is explored in Refs. [22].

In this paper we modify the approach for describing meson-baryon scattering amplitudes in the $1/N_c$ expansion, as it was applied to the case of pion photoproduction $\gamma N \rightarrow \pi N$ [23], to provide a model-independent expansion for electromagnetic multipole amplitudes of the related pion electroproduction process $e^- N \rightarrow e^- \pi N$, which at its essence is the virtual photon process $\gamma^* N \rightarrow \pi N$. Studies of $\gamma N \rightarrow \pi N$ using the more traditional “operator” approach to large N_c baryons also appear in the literature [24]. The fundamentals of hadronic electroproduction are reviewed in Ref. [25]. The photon squared four-momentum q^2 generalizes from zero in the photoproduction case to a nonzero value for electroproduction, joining the center-of-momentum (c.m.) energy W of the $\gamma^* N$ system as an independent kinematic variable for all amplitudes. Furthermore, virtual photons possess not only the familiar electric and magnetic transverse multipoles, but scalar and longitudinal multipoles as well, leading to a much richer set of experimental possibilities. Even so, the analysis of electroproduction amplitudes in the $1/N_c$ expansion is almost identical to that for the case of photoproduction. In this paper we derive expressions for pion electroproduction amplitudes at leading order (LO) and next-to-leading order (NLO) in the $1/N_c$ expansion and examine our findings using results of the MAID 2007 partial wave analysis from Universität Mainz [26].

Our purpose in this paper is to present only the results of a strict $1/N_c$ analysis. While the $1/N_c$ expansion relates combinations of distinct amplitudes and predicts the magnitude of these differences at each value of q^2 and W —an infinite number of testable predictions—it does *not* predict the shapes of their q^2 or W dependences. Obtaining such predictions would require imposing dynamical assumptions that lie beyond the raw mandates of the $1/N_c$ expansion. One may impose calculations using, for example, chiral perturbation theory, specific quark models, or generalized parton distributions on top of the amplitude predictions of this paper (granted that they have been generalized to allow for N_c to be arbitrary) to obtain predictions for the detailed q^2 and W amplitude shapes, but such modifications lie outside the intentionally limited scope of this paper. The only explicit $1/N_c$ dynamical effects we discuss below arise due to the displaced pole positions of baryon resonances in different channels.

This paper is organized as follows: In Sec. II we derive the linear electroproduction scattering amplitude relations. In Sec. III we confront the relations with the extensive results

of the MAID 2007 partial wave analysis, and comment upon the quality of the comparisons. We summarize briefly in Sec. IV.

II. DERIVATION OF LINEAR RELATIONS

Virtually all results stated in this section are a direct reprise of those for the photo-production case, Ref. [23]; the differences are particularly noted. The results for either process are obtained by starting with general meson-baryon scattering processes of the form $\Phi_1 + B_1 \rightarrow \Phi_2 + B_2$, where $\Phi_{1,2}$ are mesons and $B_{1,2}$ are baryons, each pair carrying fixed strangeness. Since the amplitude relations [8, 12] for such processes depend upon the mesons only through their quantum numbers, the same results may be used for electroproduction, for which Φ_1 is a virtual photon (or technically, a meson interpolating field with the quantum numbers of a virtual photon).

The master scattering formula for the observable scattering amplitudes $S_{L_i L_f S_i S_f I J}$ reads [8, 12]

$$\begin{aligned}
& S_{L_i L_f S_i S_f I J} \\
&= \sum_{K, \tilde{K}_i, \tilde{K}_f} [K] ([R_i] [R_f] [S_i] [S_f] [\tilde{K}_i] [\tilde{K}_f])^{1/2} \left\{ \begin{matrix} L_i & i_i & \tilde{K}_i \\ S_i & R_i & s_i \\ J & I & K \end{matrix} \right\} \left\{ \begin{matrix} L_f & i_f & \tilde{K}_f \\ S_f & R_f & s_f \\ J & I & K \end{matrix} \right\} \tau_{K \tilde{K}_i \tilde{K}_f L_i L_f},
\end{aligned} \tag{2.1}$$

where subscripts i and f label initial- and final-state quantities, respectively. Here, R indicates the baryon spin (which equals its isospin for both N and Δ), s and i label the spin and isospin of the meson (or photon), respectively, L labels the orbital angular momentum of the meson (or photon) relative to the baryon target, S labels the total spin of the system, and $\tilde{\mathbf{K}} \equiv \mathbf{i} + \mathbf{L}$ is a hybrid quantity that provides good quantum numbers \tilde{K}_i and \tilde{K}_f in the large N_c limit. The overall conserved quantum numbers I , J , and K arise from the total isospin $\mathbf{I} \equiv \mathbf{i}_i + \mathbf{R}_i = \mathbf{i}_f + \mathbf{R}_f$, the total angular momentum $\mathbf{J} \equiv \mathbf{L}_i + \mathbf{S}_i = \mathbf{L}_f + \mathbf{S}_f$, and the so-called grand spin $\mathbf{K} \equiv \mathbf{I} + \mathbf{J}$ (so that K is also a good quantum number in the large N_c limit). The braces are conventional $9j$ symbols, and the multiplicity $2X+1$ of each $SU(2)$ representation X is denoted by $[X]$. The sums run over all values of K , \tilde{K}_i , and \tilde{K}_f consistent with the nonvanishing of the $9j$ symbols, *i.e.*, each row and column satisfies the triangle rule. Beyond

all the group-theoretical factors lie the *reduced amplitudes* τ , which are the undetermined finite dynamical quantities in the large N_c scattering amplitude approach, analogous to reduced matrix elements in the Wigner-Eckart theorem; their precise calculation would be tantamount to solving QCD exactly at leading order in the $1/N_c$ expansion.

Virtual photons can carry either spin one or zero (the latter in distinction to real photons); however, the angular momentum ℓ labeling each electromagnetic multipole is comprised of the combination of the photon intrinsic spin with its orbital angular momentum relative to the target [27] (in this case, the initial baryon). In terms of Eq. (2.1), one effectively handles photon angular momentum by setting $s_i=0$ and $L_i=\ell$.

The photon isospin content is more complicated; photons carry both isovector and isoscalar contributions, which couple to baryons through operators carrying different N_c counting. Since this coupling occurs through the photon polarization vector ε_μ , and since transverse, longitudinal, and scalar polarizations (the latter two arising only for virtual photons) all have nonvanishing components in spatial ($\mu=i$) directions, the relevant operators representing photon couplings to baryons are

$$G^{ia} \equiv \sum_{\alpha=1}^{N_c} q_\alpha^\dagger \left(\frac{\sigma^i}{2} \otimes \frac{\tau^a}{2} \right) q_\alpha , \quad (2.2)$$

and

$$J^i \equiv \sum_{\alpha=1}^{N_c} q_\alpha^\dagger \left(\frac{\sigma^i}{2} \right) q_\alpha , \quad (2.3)$$

where σ and τ are Pauli matrices in spin and isospin, respectively, and α sums over the N_c quark fields q_α in the baryon. For the ground-state baryons (*e.g.*, N and Δ), matrix elements of the isoscalar operator J^i are of course $O(N_c^0)$ (since they are just components of the total baryon angular momentum), but those of the isovector operator G^{ia} are $O(N_c^1)$ due to the collective contribution of the N_c quarks. However, Eq. (2.1) does not incorporate this constraint, and therefore it must be put in by hand: The full version of Eq. (2.1) for electroproduction is the sum of a LO isovector ($i_i=1$) piece and an isoscalar ($i_i=0$) piece carrying an explicit $1/N_c$ suppression factor, as expressed below in Eqs. (2.9)–(2.11).

The master amplitude expression Eq. (2.1) applied to pion electroproduction off a nucleon target has $s_i=0$ and $L_i=\ell$ as mentioned above, as well as $i_i \equiv i_\gamma \in \{0, 1\}$, $s_f=0$, $i_f=1$ (but retaining for the moment the explicit symbol i_f), and $R_i=R_f=\frac{1}{2}$. The triangle rules

then force $S_i = S_f = \frac{1}{2}$, and we relabel $L_f \rightarrow L$, which is the pion partial wave. One finds

$$S_{\ell L \frac{1}{2} I J} = 2(-1)^{L-\ell} \sum_K [K] \left\{ \begin{array}{ccc} J & \ell & \frac{1}{2} \\ i_\gamma & I & K \end{array} \right\} \left\{ \begin{array}{ccc} J & L & \frac{1}{2} \\ i_f & I & K \end{array} \right\} \tau_{K\ell L}^\lambda. \quad (2.4)$$

Amplitudes for specific charge channels are obtained by attaching the appropriate isospin Clebsch-Gordan coefficients to Eq. (2.4). Labeling the isospin third component of the incoming nucleon by m_I and that of the outgoing pion by ν , one has

$$M_{\ell L J m_I \nu}^{\lambda i_\gamma} = 2(-1)^{L-\ell} \sum_K [K] \left\{ \begin{array}{ccc} J & \ell & \frac{1}{2} \\ i_\gamma & I & K \end{array} \right\} \left\{ \begin{array}{ccc} J & L & \frac{1}{2} \\ i_f & I & K \end{array} \right\} \tau_{K\ell L}^\lambda \\ \times \left(\begin{array}{cc|c} i_f & \frac{1}{2} & I \\ \nu & m_I - \nu & m_I \end{array} \right) \left(\begin{array}{cc|c} i_\gamma & \frac{1}{2} & I \\ 0 & m_I & m_I \end{array} \right). \quad (2.5)$$

The label λ indicates the type of multipole amplitude: $(\ell - L)$ odd gives electric (e), longitudinal (l), and scalar (s) multipoles (the latter two being absent from photoproduction), and $(\ell - L)$ even gives magnetic (m) multipoles. The l and s multipoles are linearly dependent due to current conservation [25], so we choose in this analysis to eliminate l multipoles in favor of s multipoles.

We now exploit the result that amplitudes with $|I_t - J_t| = n$ are suppressed by a relative factor $1/N_c^n$. The first step is to rewrite the $9j$ symbols in Eq. (2.1) in terms of t -channel quantum numbers using the well-known SU(2) relation known as the Biedenharn-Elliott sum rule [28]. In terms of modified $6j$ symbols (called $[6j]$ symbols in Ref. [21]),

$$\left\{ \begin{array}{ccc} a & b & e \\ c & d & f \end{array} \right\} \equiv \frac{(-1)^{-(b+d+e+f)}}{([a][b][c][d])^{1/4}} \left[\begin{array}{ccc} a & b & e \\ c & d & f \end{array} \right], \quad (2.6)$$

one obtains

$$\left\{ \begin{array}{ccc} J & \ell & \frac{1}{2} \\ i_\gamma & I & K \end{array} \right\} \left\{ \begin{array}{ccc} J & L & \frac{1}{2} \\ i_f & I & K \end{array} \right\} = \sum_{\mathcal{J}} \frac{(-1)^{2\mathcal{J}-i_f+i_\gamma} [\mathcal{J}]}{2\sqrt{[i_f][i_\gamma][L][\ell]}} \left[\begin{array}{ccc} i_f & L & K \\ \ell & i_\gamma & \mathcal{J} \end{array} \right] \left[\begin{array}{ccc} i_f & \frac{1}{2} & I \\ \frac{1}{2} & i_\gamma & \mathcal{J} \end{array} \right] \left[\begin{array}{ccc} L & \frac{1}{2} & J \\ \frac{1}{2} & \ell & \mathcal{J} \end{array} \right], \quad (2.7)$$

where the quantum number \mathcal{J} clearly adopts the role of both I_t (as seen from the second $[6j]$ symbol) and J_t (as seen from the third). Setting at last $i_f = 1$ and defining the t -channel reduced amplitudes by

$$\tau_{\mathcal{J}\ell L}^{t\lambda i_\gamma} \equiv \frac{(-1)^{2\mathcal{J}-1+i_\gamma} [\mathcal{J}]}{\sqrt{[1][i_\gamma][L][\ell]}} \sum_K [K] \left[\begin{array}{ccc} 1 & L & K \\ \ell & i_\gamma & \mathcal{J} \end{array} \right] \tau_{K\ell L}^\lambda, \quad (2.8)$$

one obtains the multipoles for the isovector case ($i_\gamma = 1$):

$$M_{\ell L J m_I \nu}^{\lambda I 1} = (-1)^{L-\ell} \begin{pmatrix} 1 & \frac{1}{2} & I \\ \nu & m_I - \nu & m_I \end{pmatrix} \begin{pmatrix} 1 & \frac{1}{2} & I \\ 0 & m_I & m_I \end{pmatrix} \sum_{\mathcal{J}} \begin{bmatrix} 1 & \frac{1}{2} & I \\ \frac{1}{2} & 1 & \mathcal{J} \end{bmatrix} \begin{bmatrix} L & \frac{1}{2} & J \\ \frac{1}{2} & \ell & \mathcal{J} \end{bmatrix} \tau_{\mathcal{J} \ell L}^{t \lambda 1}, \quad (2.9)$$

and those for isoscalar case ($i_\gamma = 0$):

$$M_{\ell L J m_I \nu}^{\lambda I 0} = \frac{(-1)^{L-\ell}}{N_c} \begin{pmatrix} 1 & \frac{1}{2} & \frac{1}{2} \\ \nu & m_I - \nu & m_I \end{pmatrix} \frac{\delta_{I, \frac{1}{2}}}{[1]^{1/4}} \begin{bmatrix} L & \frac{1}{2} & J \\ \frac{1}{2} & \ell & 1 \end{bmatrix} \tau_{1 \ell L}^{t \lambda 0}. \quad (2.10)$$

Note the explicit $1/N_c$ suppression factor in the isoscalar expression. In order to achieve relations at a consistent order in the $1/N_c$ expansion, one must also include the independent NLO isovector amplitudes, which have $|I_t - J_t| = 1$. Generalizing Eq. (2.9) gives

$$M_{\ell L J m_I \nu}^{\lambda I 1(\text{NLO})} = \frac{(-1)^{L-\ell}}{N_c} \begin{pmatrix} 1 & \frac{1}{2} & I \\ \nu & m_I - \nu & m_I \end{pmatrix} \begin{pmatrix} 1 & \frac{1}{2} & I \\ 0 & m_I & m_I \end{pmatrix} \\ \times \left\{ \sum_x \begin{bmatrix} 1 & \frac{1}{2} & I \\ \frac{1}{2} & 1 & x \end{bmatrix} \begin{bmatrix} L & \frac{1}{2} & J \\ \frac{1}{2} & \ell & x+1 \end{bmatrix} \tau_{x \ell L}^{t \lambda(+)} + \sum_y \begin{bmatrix} 1 & \frac{1}{2} & I \\ \frac{1}{2} & 1 & y \end{bmatrix} \begin{bmatrix} L & \frac{1}{2} & J \\ \frac{1}{2} & \ell & y-1 \end{bmatrix} \tau_{y \ell L}^{t \lambda(-)} \right\}, \quad (2.11)$$

where x in the first sum and y in the second represent I_t , and the amplitudes $\tau^{t \lambda(\pm)}$ are independent of those at leading order. The total multipole amplitude, including LO and NLO terms to consistent order in $1/N_c$, is therefore the sum of Eqs. (2.9), (2.10), and (2.11):

$$M_{\ell L J m_I \nu}^{\lambda I} = M_{\ell L J m_I \nu}^{\lambda I 1} + M_{\ell L J m_I \nu}^{\lambda I 0} + M_{\ell L J m_I \nu}^{\lambda I 1(\text{NLO})}. \quad (2.12)$$

By including all values of \mathcal{J} , x , and y allowed by the triangle rules in the [6j] symbols and simplifying, one obtains the expression

$$M_{\ell L J}^{\lambda m_I \nu} = \sum_I (-1)^{L-\ell} \begin{pmatrix} 1 & \frac{1}{2} & I \\ \nu & m_I - \nu & m_I \end{pmatrix} \left[\begin{pmatrix} 1 & \frac{1}{2} & I \\ 0 & m_I & m_I \end{pmatrix} \right. \\ \times \left\{ \delta_{\ell, L} \tau_{0 L L}^{t \lambda 1} + \sqrt{\frac{2}{3}} \left(\delta_{I, \frac{1}{2}} - \frac{1}{2} \delta_{I, \frac{3}{2}} \right) \begin{bmatrix} L & \frac{1}{2} & J \\ \frac{1}{2} & \ell & 1 \end{bmatrix} \tau_{1 \ell L}^{t \lambda 1} \right. \\ \left. + \frac{1}{N_c} \left(\begin{bmatrix} L & \frac{1}{2} & J \\ \frac{1}{2} & \ell & 1 \end{bmatrix} \tau_{0 \ell L}^{t \lambda(+)} + \sqrt{\frac{2}{3}} \left(\delta_{I, \frac{1}{2}} - \frac{1}{2} \delta_{I, \frac{3}{2}} \right) \delta_{\ell, L} \tau_{1 L L}^{t \lambda(-)} \right) \right\} \\ \left. + \frac{1}{N_c} \frac{\delta_{I, \frac{1}{2}}}{[1]^{1/4}} \begin{bmatrix} L & \frac{1}{2} & J \\ \frac{1}{2} & \ell & 1 \end{bmatrix} \tau_{1 \ell L}^{t \lambda 0} \right], \quad (2.13)$$

which is identical in form to the expression found for photoproduction [23].

Pion electroproduction possesses four charged channels: $\gamma^*p \rightarrow \pi^+n$, $\gamma^*n \rightarrow \pi^-p$, $\gamma^*p \rightarrow \pi^0p$ and $\gamma^*n \rightarrow \pi^0n$. Assuming isospin invariance, only three of these are independent [25], and so we choose to eliminate the channel $\gamma^*n \rightarrow \pi^0n$ for which all the particles are neutral. Since the initial- and final-state nucleons carry only spin 1/2, parity invariance constrains electric and scalar multipole amplitudes to $\ell = L \pm 1$, while magnetic multipole amplitudes satisfy $\ell = L$. The spinless pion and spin-1/2 nucleon combine to give possible angular momenta $J = L \pm \frac{1}{2}$; it is convenient to express this information using the combination $2(J-L)$, which equals ± 1 for $J = L \pm \frac{1}{2}$, respectively, and write the amplitudes as $M_{\ell,L,2(J-L)}^\lambda$. Using the conventions [25] employed by MAID, the multipole amplitude $M_{\ell,L,2(J-L)}^\lambda$ (where $\lambda = e, s, \text{ or } m$) is proportional to $\Lambda_{L,2(J-L)}$; for example, $M_{L-1,L,-}^s \propto S_{L-}$. The proportionality factor depends upon particle energies, λ , L , and $2(J-L)$, but is not important for this analysis since in each relation presented below it cancels out as a common factor.

Using Eq. (2.13), one obtains very similar relations for electric and scalar multipoles:

$$M_{L-1,L,-}^{e/s,p(\pi^+)n} = M_{L-1,L,-}^{e/s,n(\pi^-)p} + O(N_c^{-1}) \quad (L \geq 2 \text{ for } e, L \geq 1 \text{ for } s), \quad (2.14)$$

$$M_{L+1,L,+}^{e/s,p(\pi^+)n} = M_{L+1,L,+}^{e/s,n(\pi^-)p} + O(N_c^{-1}) \quad (L \geq 0), \quad (2.15)$$

and

$$M_{L\pm 1,L,\pm}^{e/s,p(\pi^0)p} = O(N_c^{-1}). \quad (2.16)$$

The presence of an $L=1$ relation for s but not e amplitudes in Eq. (2.14) reflects the existence of C0 but not E0 electromagnetic multipoles. Referring to Eq. (2.13), one obtains four relations at LO because one has six observable amplitudes, arising through three charged channels each with two allowed values of $2(J-L)$, but only two reduced amplitudes, $\tau_{1,L\pm 1,L}^{te/s1}$. However, no relations survive at NLO because four new amplitudes ($\tau_{0,L\pm 1,L}^{te/s(+)}$ and $\tau_{1,L\pm 1,L}^{te/s0}$) appear at this order. Equation (2.16) implies the vanishing of the e and s multipole amplitudes at LO for the process $\gamma^*p \rightarrow \pi^0p$, which means that they are expected to be, on average, a factor of about $N_c = 3$ smaller than the charged amplitudes; but this is a rather qualitative statement [in particular, Eq. (2.16) does not test the equality of measurable amplitudes], and we omit numerical analysis of such amplitudes below.

Using Eq. (2.13) for the magnetic multipole amplitudes, one again has six observable amplitudes expressed at LO in terms of only two reduced amplitudes (τ_{1LL}^{tm1} and τ_{0LL}^{tm1}), leading to four relations:

$$M_{L,L,-}^{m,p(\pi^0)p} = M_{L,L,+}^{m,p(\pi^0)p} + O(N_c^{-1}) \quad (L \geq 1), \quad (2.17)$$

$$M_{L,L,-}^{m,p(\pi^+)n} = M_{L,L,-}^{m,n(\pi^-)p} = -\frac{L+1}{L} M_{L,L,+}^{m,p(\pi^+)n} = -\frac{L+1}{L} M_{L,L,+}^{m,n(\pi^-)p} + O(N_c^{-1}) \quad (L \geq 1). \quad (2.18)$$

Only three new reduced amplitudes ($\tau_{0LL}^{tm(+)}$, $\tau_{1LL}^{tm(-)}$, and τ_{1LL}^{tm0}) appear at NLO, meaning that one special combination holds at both LO and NLO:

$$M_{L,L,-}^{m,p(\pi^+)n} = M_{L,L,-}^{m,n(\pi^-)p} - \left(\frac{L+1}{L}\right) \left[M_{L,L,+}^{m,p(\pi^+)n} - M_{L,L,+}^{m,n(\pi^-)p} \right] + O(N_c^{-2}) \quad (L \geq 1). \quad (2.19)$$

One expects this relation to improve generically upon the predictions of the LO relations by a factor of about $N_c=3$.

Note that several of the LO relations, specifically those of the form $M_{\ell,L,\pm}^{\lambda,p(\pi^+)n} = M_{\ell,L,\pm}^{\lambda,n(\pi^-)p}$ [which are Eqs. (2.14)–(2.15) and the first and third of relations in Eq. (2.18)] follow directly from isospin symmetry and the LO dominance of the isovector amplitude, as may be checked simply from the Clebsch-Gordan coefficients in Eq. (2.9). All of the electroproduction multipole relations presented here also appear for the photoproduction, of course excepting the scalar multipole relations.

III. RESULTS

Our results consist of a comparison of the relations Eqs. (2.14)–(2.15) and (2.17)–(2.19) to the experimental data as obtained from the MAID 2007 partial-wave analysis [26]. The exceptionally large volume of available information is presented as concisely as possible: Each allowed partial wave [L can be arbitrarily large, and Eqs. (2.14)–(2.19) provide relations between such amplitudes, but data is typically compiled only up to $L = 5$] is a complex-valued amplitude and depends upon two independent dynamical variables: the photon virtuality $Q^2 \equiv -q^2$ and the γ^*N c.m. energy W . In each plot W ranges from threshold to 2 GeV, and Q^2 ranges from 0–5 GeV². In all figures we present both real and imaginary parts of the

left-hand and right-hand sides (l.h.s. and r.h.s.) of each multipole amplitude combination appearing in Eqs. (2.14)–(2.15) and (2.17)–(2.19) (except for $L = 4$ and 5 imaginary parts, given as zero by MAID), and then also plot scale-independent amplitude ratios according to the prescription

$$\text{Ratio} = \frac{\text{l.h.s.} - \text{r.h.s.}}{\frac{1}{2}(|\max(\text{l.h.s.})| + |\max(\text{r.h.s.})|)}. \quad (3.1)$$

For a LO relation, this quantity is dimensionless and predicted to be of order $1/N_c$, while for NLO relations the prediction is $O(1/N_c^2)$. Absolute values appear in the denominator to avoid physically uninteresting behavior when l.h.s. and r.h.s. are both near zero and happen to be equal and opposite. Maximally poor relationships ($|\text{l.h.s.}| \gg |\text{r.h.s.}|$ or vice versa) are manifested by $\text{Ratio} \rightarrow \pm 2$. On the other hand, relations that truly hold to $O(1/N_c)$ might be expected to lie between $\pm 1/3$; however, this conclusion neglects the order-unity coefficient implicit in $O(1/N_c)$. We choose as a useful metric to distinguish between $O(1/N_c)$ and $O(N_c^0)$ quantities their geometric mean, $\pm 1/N_c^{1/2} \approx \pm 0.577$ for $N_c = 3$. Similarly, we take the largest $O(1/N_c^2)$ effects to be $\pm 1/N_c^{3/2} \approx \pm 0.192$; nevertheless, the reader is free to choose their own figure of merit upon viewing the plots.

Figure 1 tests the e multipole relations in Eq. (2.14), which compare amplitudes with $J = L - 1/2$, denoted as E_{L-} by MAID. Figure 2 does the same for S_{L-} multipoles. The $J = L + 1/2$ amplitudes for e and s [relations in Eq. (2.15) for multipoles E_{L+} and S_{L+}] appear in Figs. 3 and 4, respectively. The m multipole relations Eq. (2.17) containing a π^0 and relating $J = L \pm 1/2$ amplitudes ($M_{L\pm}$) appear in Fig. 5. All of the relations presented in these first figures are LO in the $1/N_c$ expansion. Figure 6 tests the m multipole relations containing π^\pm , first for the M_{L-} multipoles alone [the LO relation represented by the first expression in Eq. (2.18)] and then for the NLO relation between $M_{L\pm}$ multipoles given in Eq. (2.19). We remind the reader that the relations explored in Figs. 1–4 and the LO comparisons of Fig. 6 are dominated by the isovector component of the photon.

First observe that the limit $Q^2 \rightarrow 0$ corresponds to scattering with an on-shell photon, *i.e.*, real pion photoproduction. The projection of each e and m multipole on the Q^2 axis gives amplitude curves obtained in Ref. [23] and analyzed there in terms of the multipole relations Eqs. (2.14)–(2.15) and (2.17)–(2.19) restricted to $Q^2 = 0$.

The most prominent features in the amplitudes are of course the baryon resonances, which are most apparent through large enhancements of the imaginary parts at values of

c.m. energy W equal to a resonance mass, but also noticeable from points where the real parts vanish. The falloff of each amplitude with increasing Q^2 may be interpreted as the canonical behavior of an NN^* electromagnetic transition form factor, with the on-shell photon ($Q^2 = 0$) providing the least disruptive probe of the initial nucleon and hence the most efficient probe for producing a resonance. One finds, however, interesting exceptions to this reasoning; in the imaginary part of the S_{2-} amplitudes (Fig. 2), one sees that the $N(1520)$ produced in $\gamma^*p \rightarrow \pi^+n$ (l.h.s.) peaks at $Q^2 = 0$, while that in $\gamma^*n \rightarrow \pi^-p$ (r.h.s.) peaks at $Q^2 = 0.6 \text{ GeV}^2$.

The resonant behavior accounts for the largest source of discrepancies of the $1/N_c$ relations. Often one finds resonant behavior on both sides of a given relation, but with greatly differing residues at the peak; this is the case for the $N(1680)$ peak in each E_{3-} amplitude of Fig. 1 or each S_{3-} amplitude of Fig. 2. Even the sign of the $N(1720)$ residue is different between the two E_{1+} amplitudes in Fig. 3, while the $N(1720)$ appears to be absent altogether from the r.h.s. plot for S_{1+} in Fig. 4 although the amplitudes otherwise appear very similar. These are interesting anomalies arising even in amplitudes for which the value of J on both sides of the amplitude relation are the same, so that the same resonance (or more accurately, different members of an isomultiplet) appears on both sides. For Fig. 5 and the NLO relation of Fig. 6, J differs on the two sides of the equation, meaning that distinct resonances appear. In the $L = 1$ amplitudes of Fig. 5, for example, the $N(1440)$ resonance appearing in the M_{1-} (l.h.s.) amplitude is broad and shallow, while the $\Delta(1232)$ forms a huge peak in the M_{1+} (r.h.s.) amplitude, with just a hint of the $N(1440)$'s true large- N_c partner [12], the $\Delta(1600)$, perhaps just visible.

In fact, the $\Delta(1232)$ should be eliminated from a large N_c analysis of baryon resonances, because it is actually a degenerate partner to the nucleon whose width vanishes as $N_c \rightarrow \infty$, unlike the true resonances whose widths remain finite in this limit [13]. It is only due to the numerical accident that the chiral limit ($m_\pi \rightarrow 0$) is more closely achieved in our $N_c = 3$ universe than is the $1/N_c \rightarrow 0$ limit [17] that the $\Delta(1232)$ in our universe decays to πN . However, true resonant “shifted degenerate” pairs such as $N(1440)$ and $\Delta(1600)$ are particularly interesting because their masses differ by an amount that is $O(1/N_c^2)$ relative to their average [12], about 100–150 MeV. Another example of this effect appears in the $L = 2$ amplitudes in Fig. 5, with the $N(1520)$ [and perhaps also the $N(1700)$ or $\Delta(1700)$] appearing in the M_{2-} (l.h.s.) and $N(1675)$ with a much smaller residue appearing in the

M_{2+} (r.h.s.). In fact, precisely the pair of $N(1520)$ and $N(1675)$ are considered as degenerate resonances in Ref. [23], where it is shown that the on-resonance couplings for the different channels behave exactly as expected from the $1/N_c$ expansion for $N_c=3$. Another “shifted degenerate” pair in Fig. 5 appears to be $N(1680)$ in the M_{3-} (l.h.s.) amplitude and $\Delta(1950)$ in the M_{3+} (r.h.s.) amplitude; the $\Delta(1950)$ is not apparent in the plots of Ref. [23], which employs the older MAID 2003 analysis rather than the MAID 2007 variant used here.

In the case of the NLO relations Eq. (2.19) considered in Fig. 6, the LO terms are M_{L-} and the NLO terms are M_{L+} , so entirely new resonances can appear at NLO. A curious example occurs for $L=1$; the broad peak appearing for $\gamma^*p \rightarrow \pi^+n$ (l.h.s.), probably due to the $N(1440)$, is unmatched by a contribution in $\gamma^*n \rightarrow \pi^-p$ in the M_{1-} amplitudes, and moreover, the $N(1720)$ appears prominently in the M_{1+} NLO corrections. On the other hand, the NLO contributions sometimes indicate a shifted degenerate pair; this effect occurs for the already-mentioned $N(1520)$ and $N(1675)$ pair occurring at $L=2$ [23].

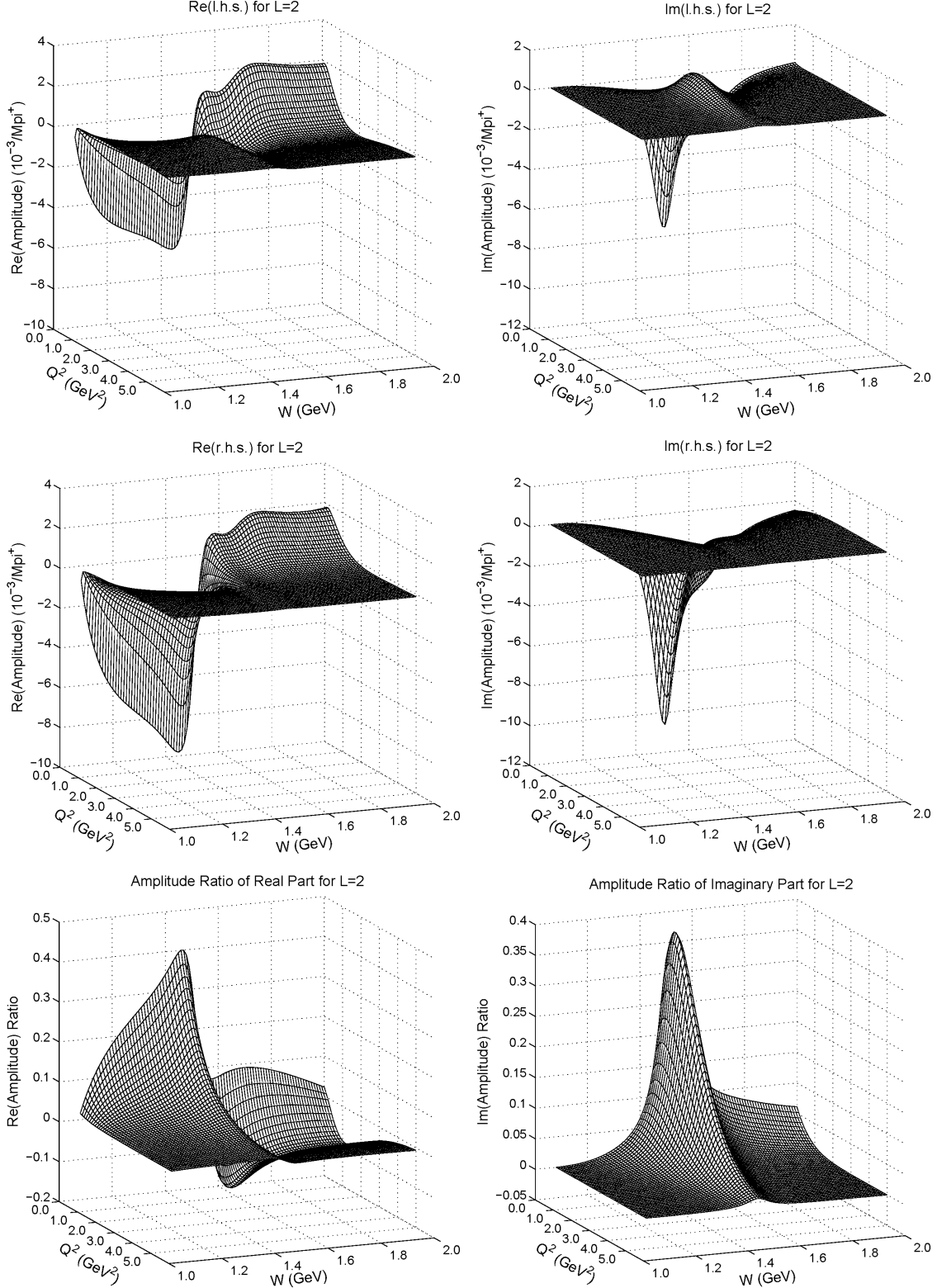
In regions away from resonances and for amplitudes not exhibiting any obvious resonances, the agreement tends to be rather better. This is certainly true for the $L=4$ and 5 amplitudes, but also for larger values of Q^2 and for values of W close to threshold as well as values at least 50–100 MeV from resonant peaks. Of the highest quality are the isovector-dominated relations in Figs. 1–4, for which the same value of J appearing on either side of the equation means that resonances appearing on the two sides of the relation belong to an isomultiplet. On the other hand, the benefits of the NLO correction in Fig. 6 remain ambiguous; for example, some improvement appears in the real part of the $L=1$ relation, but the quality degrades in some kinematic regions for $L=2$, and scarcely any change due to the NLO terms is noticeable for $L \geq 3$.

IV. CONCLUSIONS

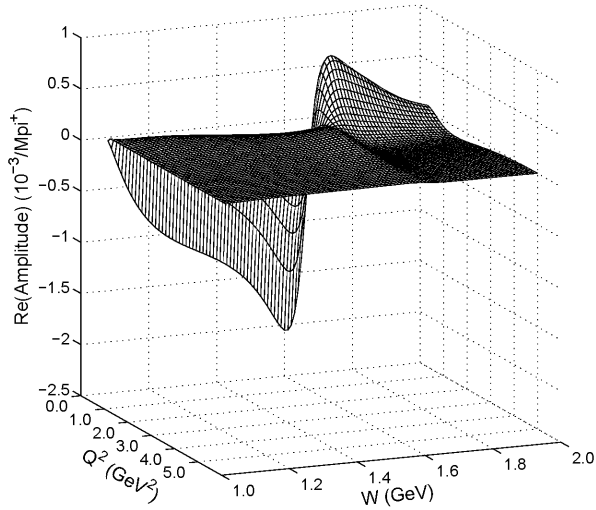
The $1/N_c$ expansion, which has provided so much qualitative and semiquantitative guidance to understanding baryons in general, and the baryon resonance spectrum in particular, appears in the case of electroproduction to produce more ambiguous results. On one hand, it gives a natural explanation for the dominance of isovector over isoscalar amplitudes, and it provides a definite set of linear relations between multipole amplitudes that are expected to hold at all values of c.m. energy W and photon virtuality Q^2 . For values of W not near

resonance masses as well as for larger values of Q^2 , the agreement tends to be in accordance with the expectations of the $1/N_c$ expansion. Even in the resonant region, one often sees evidence of the “shifted degenerate” resonances carrying different quantum numbers [such as $N(1520)$ and $N(1675)$] that have related couplings. However, just as many cases exist in which the amplitudes in the resonant region do not entirely conform to naive $1/N_c$ expectations, both at leading and subleading order. The specific reason that a given large N_c relation for pion electroproduction works surprisingly well or surprisingly poorly in the resonant region remains a challenge for future research.

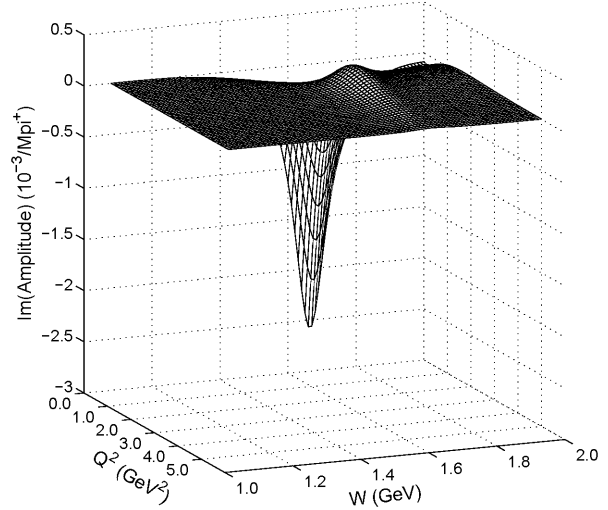
FIG. 1: Electric multipole data ($J = L - \frac{1}{2}$ amplitudes E_{L-}) from MAID 2007. The l.h.s., r.h.s., and ratio of relation (2.14) for $L \geq 2$ are presented in separate rows, with separate columns for the real and imaginary parts (except for the $L = 4$ and 5 imaginary parts, given as zero by MAID).



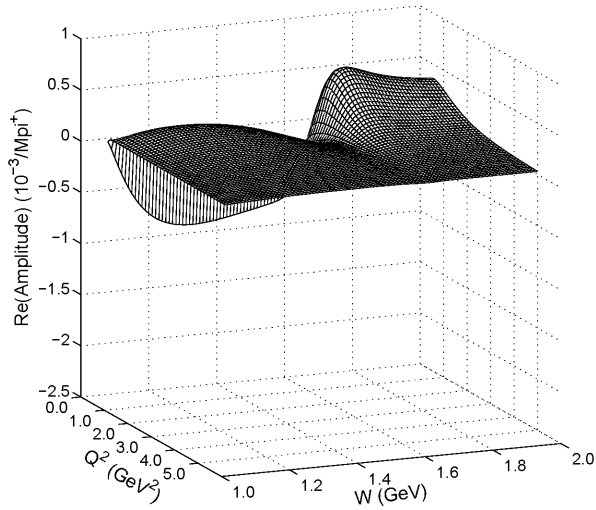
Re(l.h.s.) for L=3



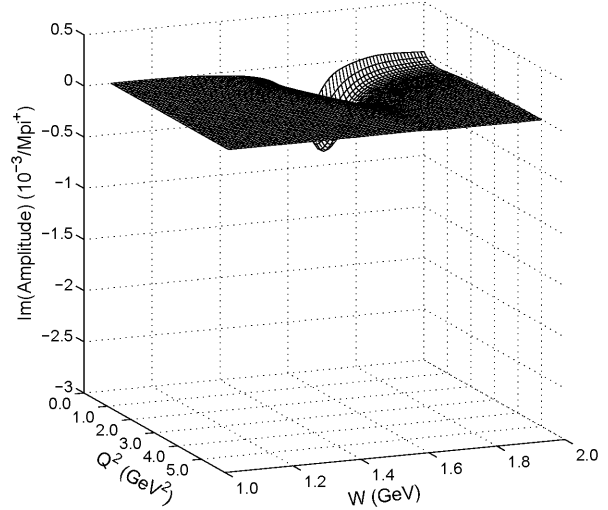
Im(l.h.s.) for L=3



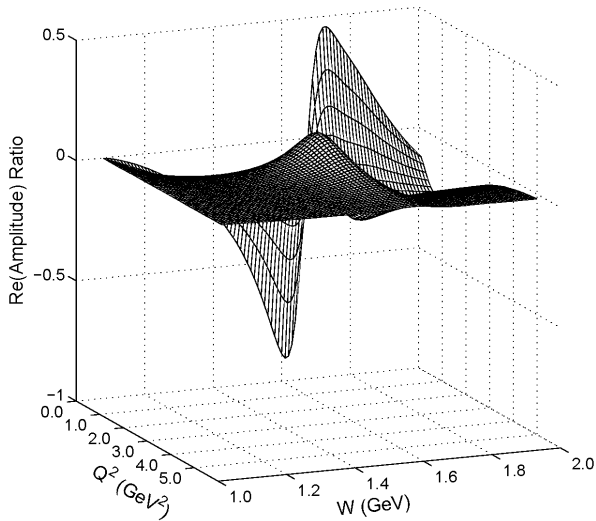
Re(r.h.s.) for L=3



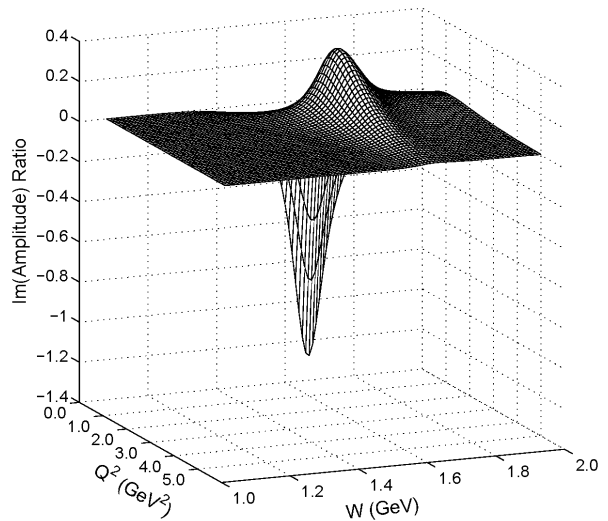
Im(r.h.s.) for L=3



Amplitude Ratio of Real Part for L=3



Amplitude Ratio of Imaginary Part for L=3



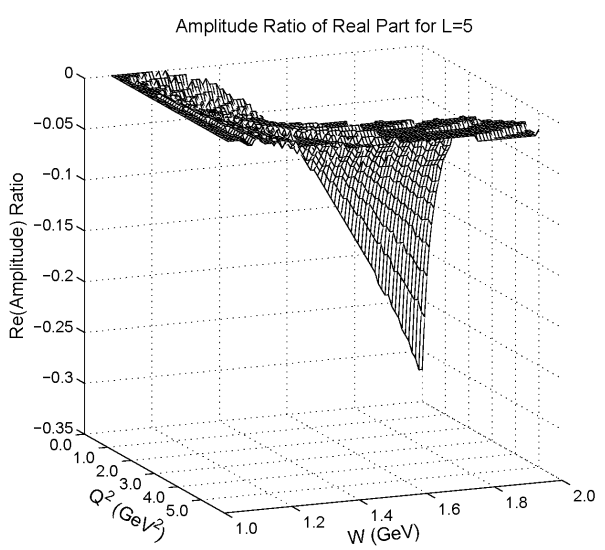
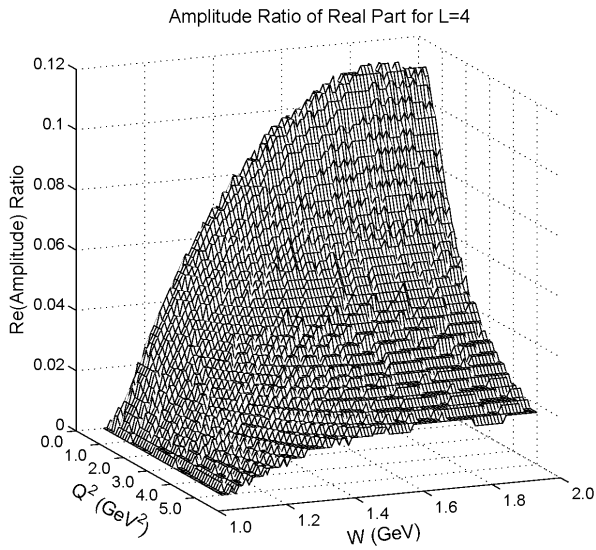
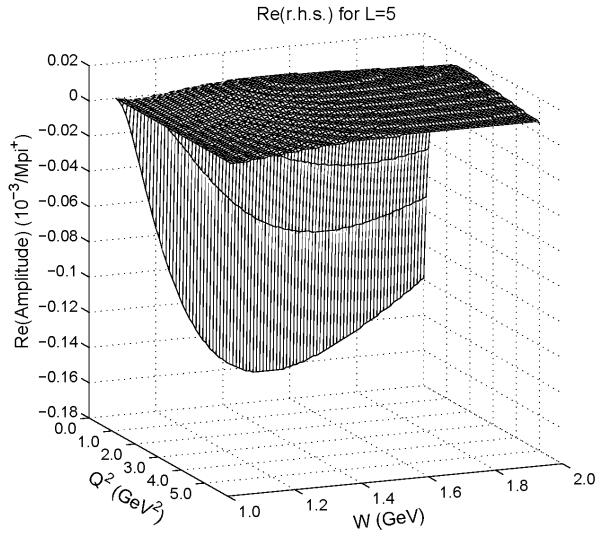
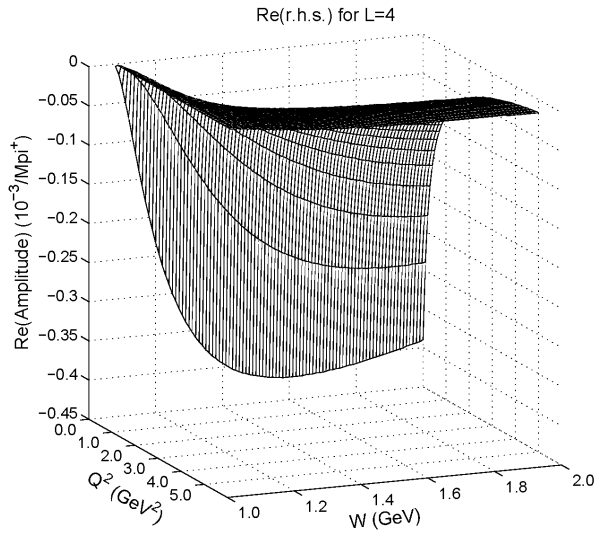
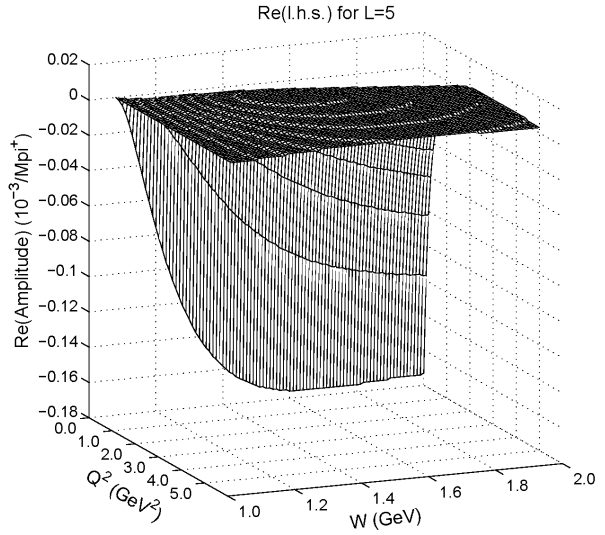
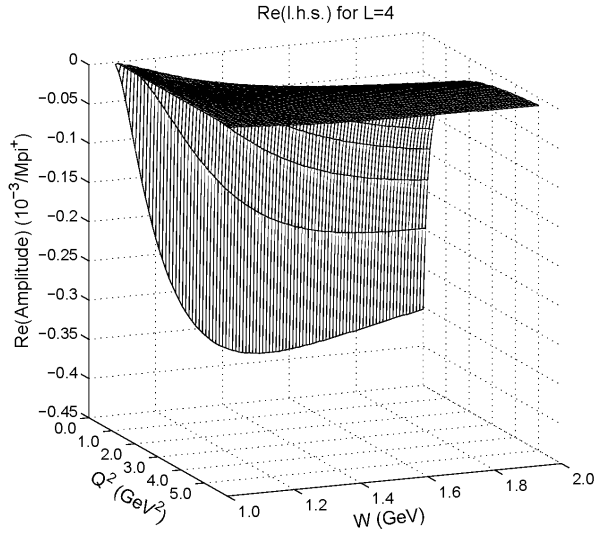
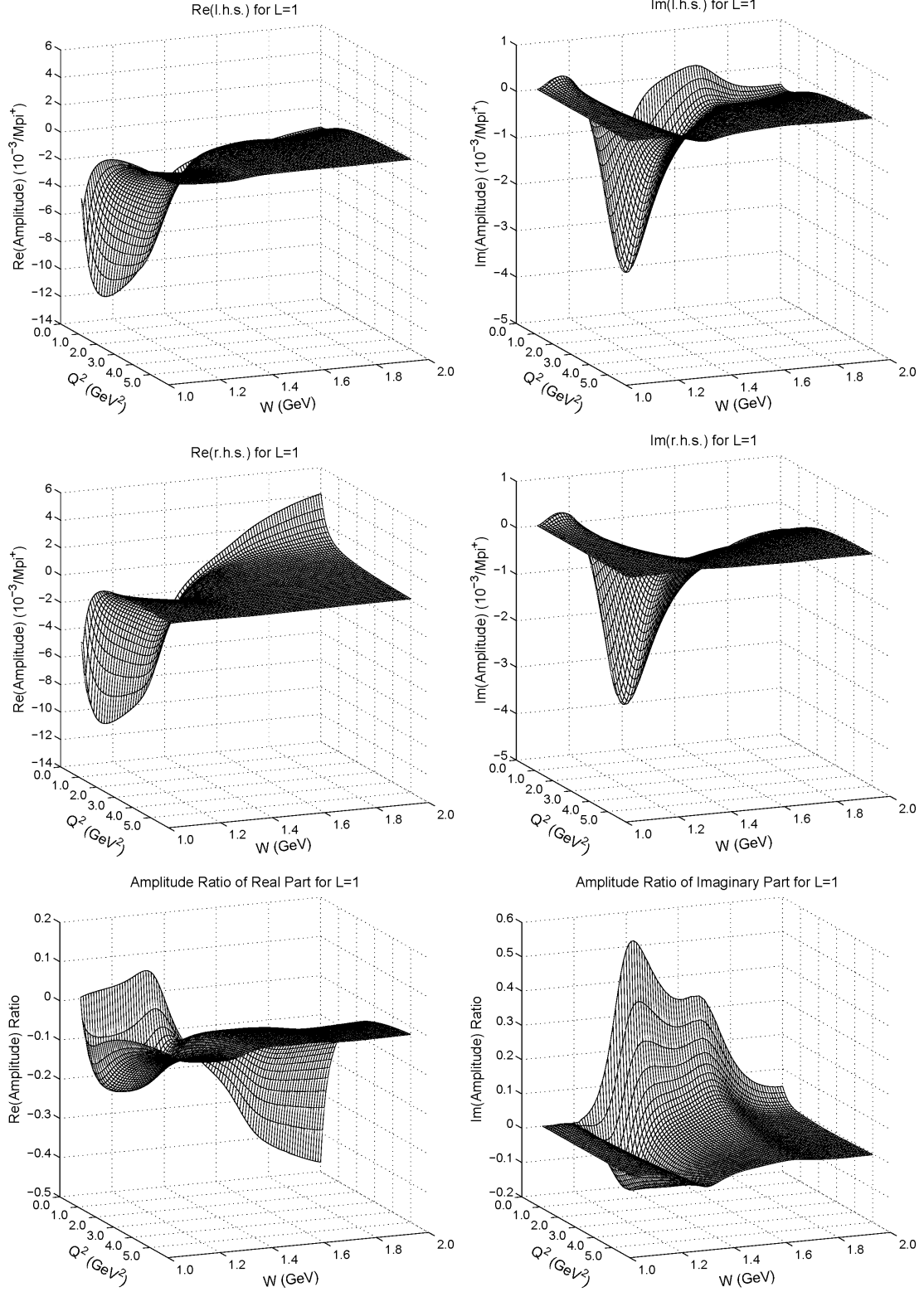
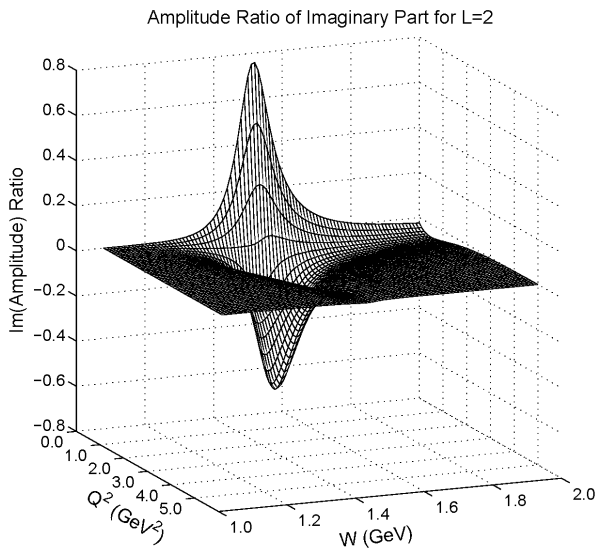
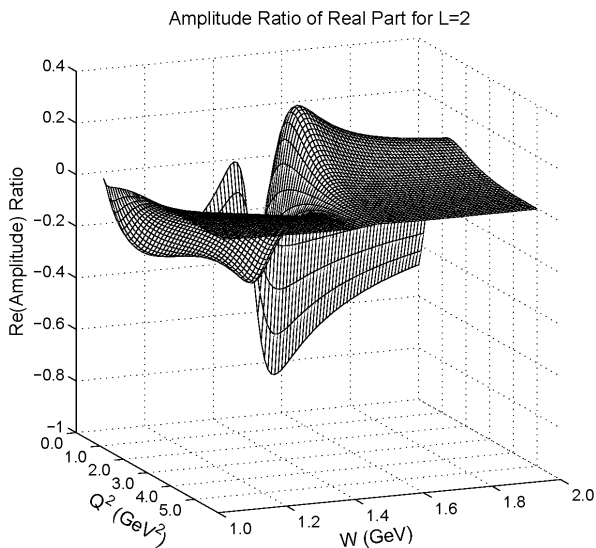
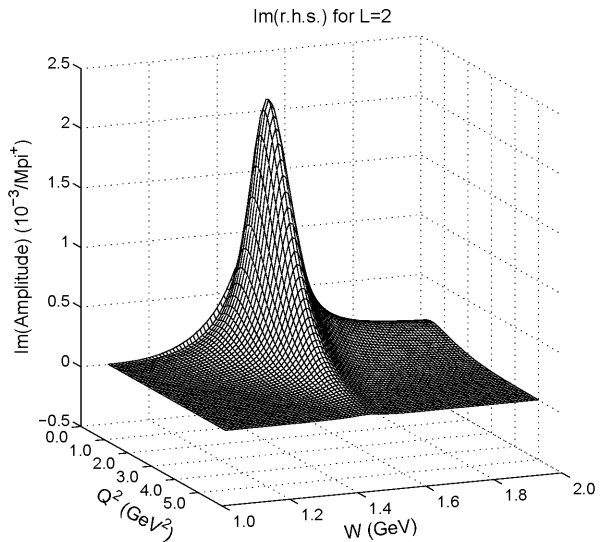
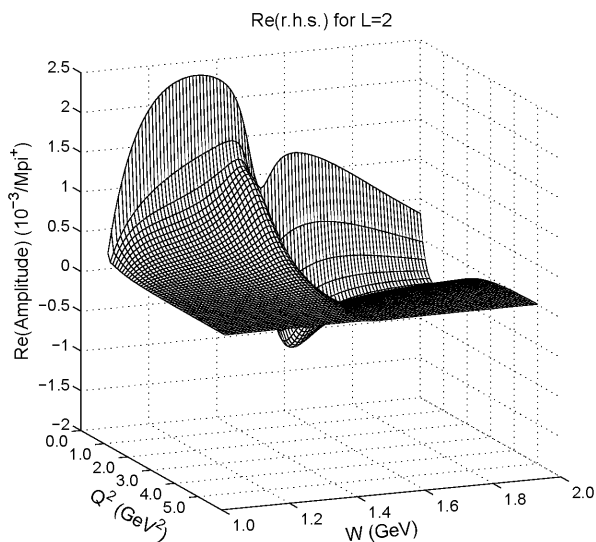
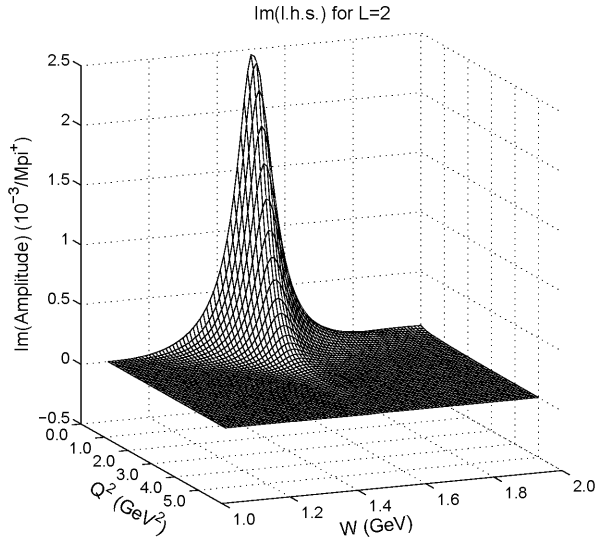
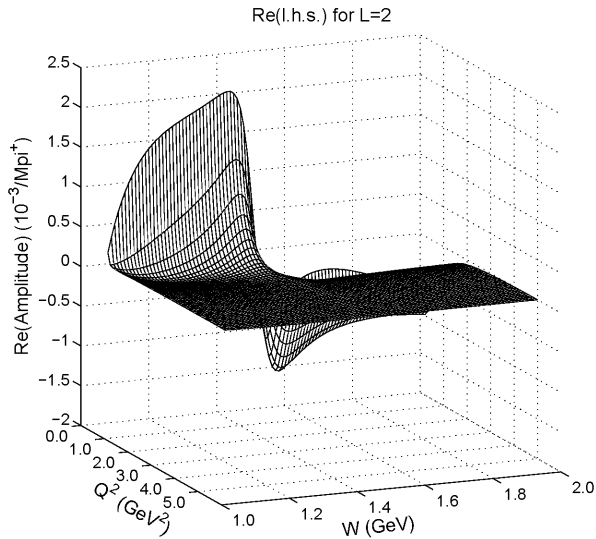
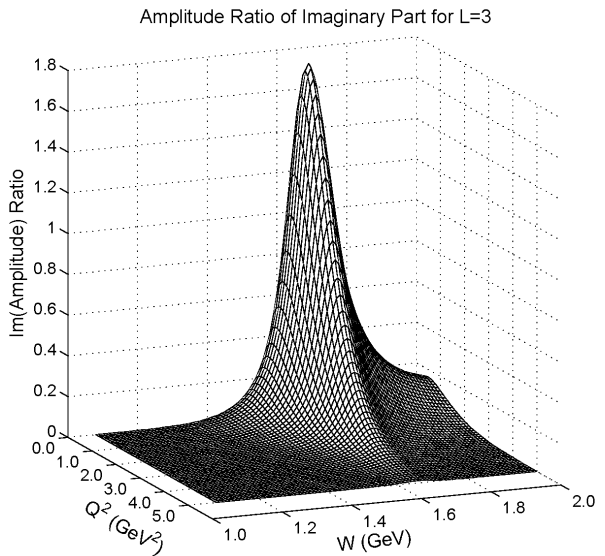
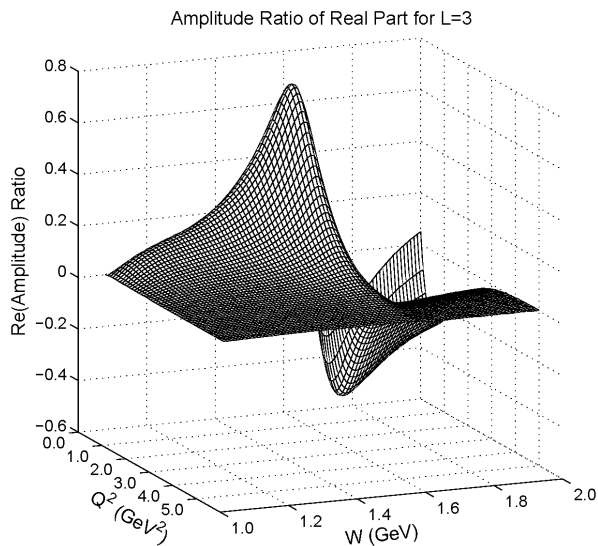
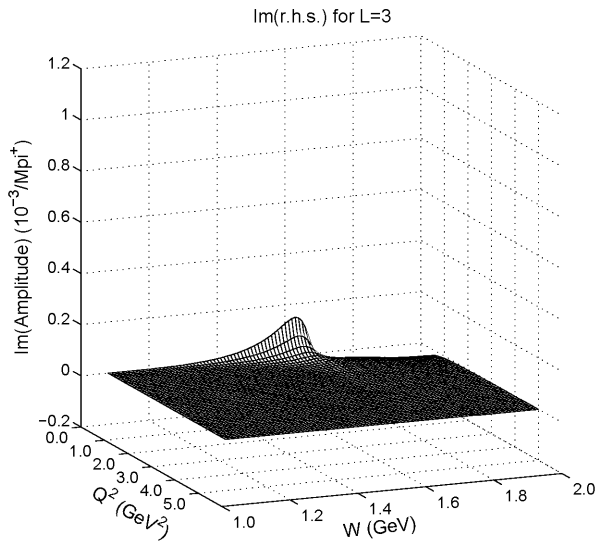
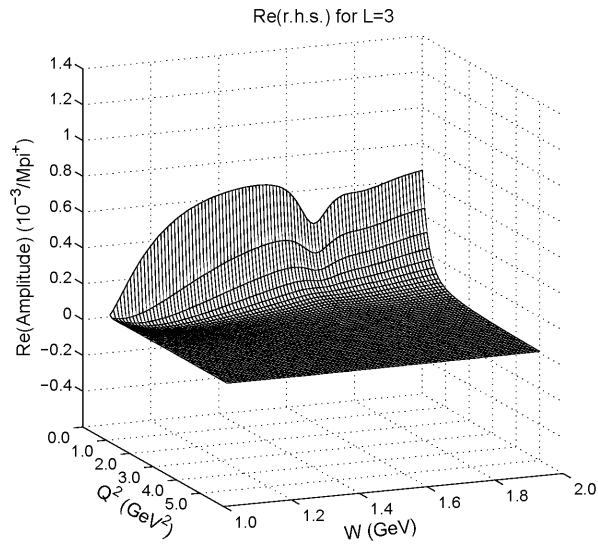
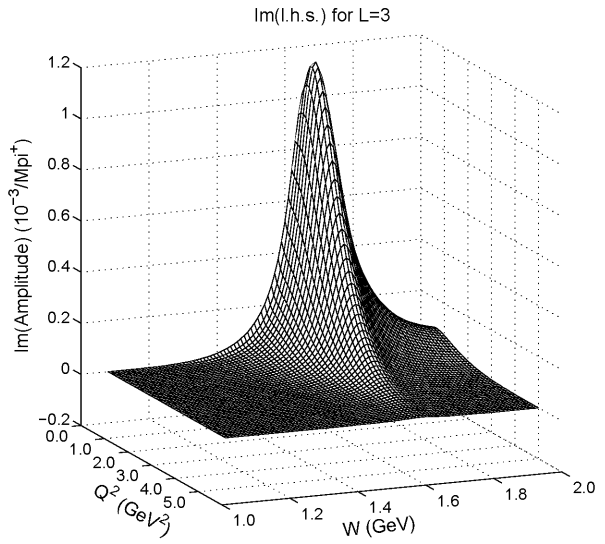
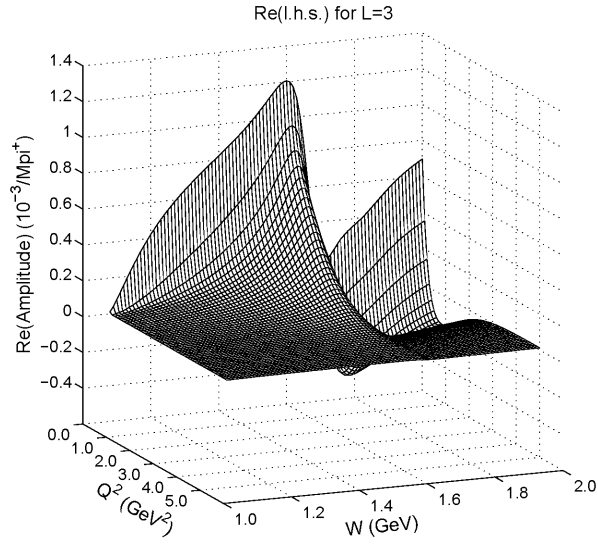


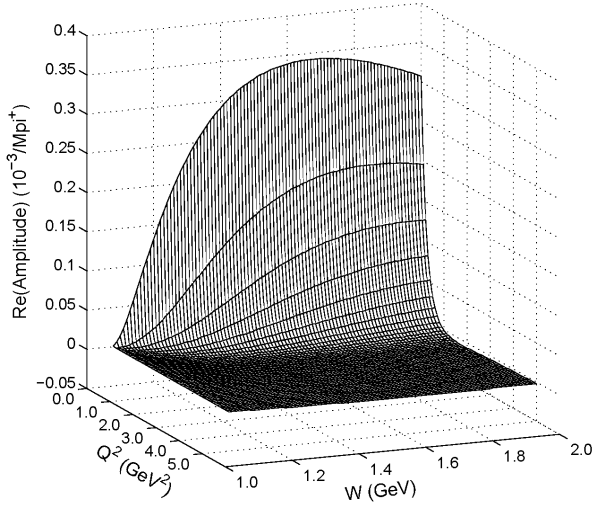
FIG. 2: Scalar multipole data ($J = L - \frac{1}{2}$ amplitudes S_{L-}) from MAID 2007. The l.h.s., r.h.s., and ratio of relation (2.14) for $L \geq 1$ are presented in separate rows, with separate columns for the real and imaginary parts (except for the $L = 4$ and 5 imaginary parts, given as zero by MAID).



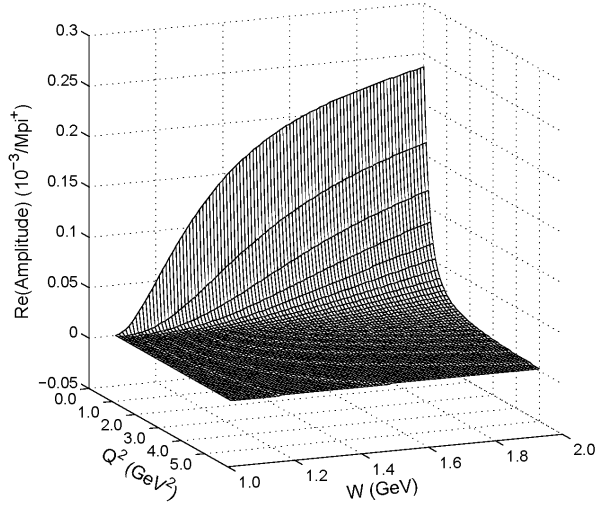




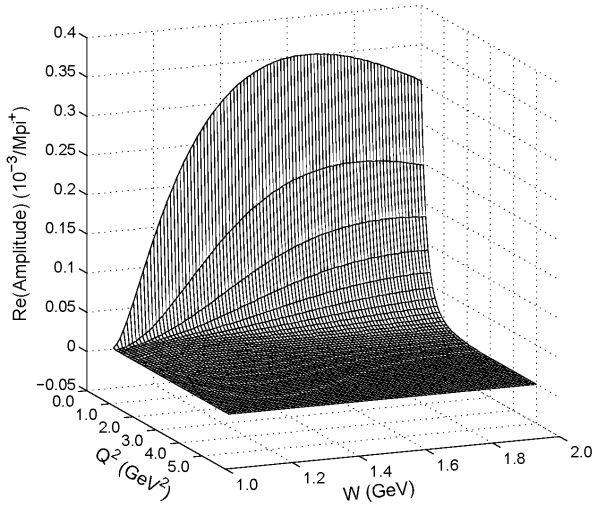
Re(l.h.s.) for L=4



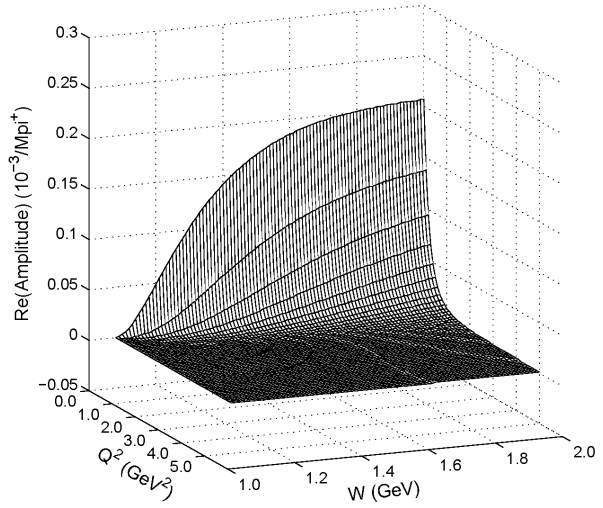
Re(l.h.s.) for L=5



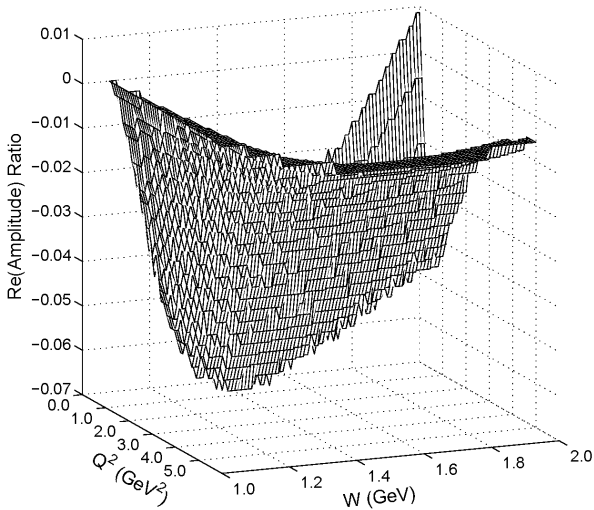
Re(r.h.s.) for L=4



Re(r.h.s.) for L=5



Amplitude Ratio of Real Part for L=4



Amplitude Ratio of Real Part for L=5

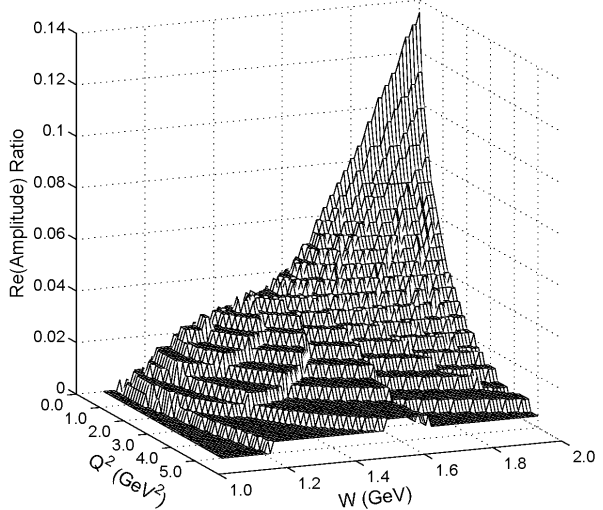
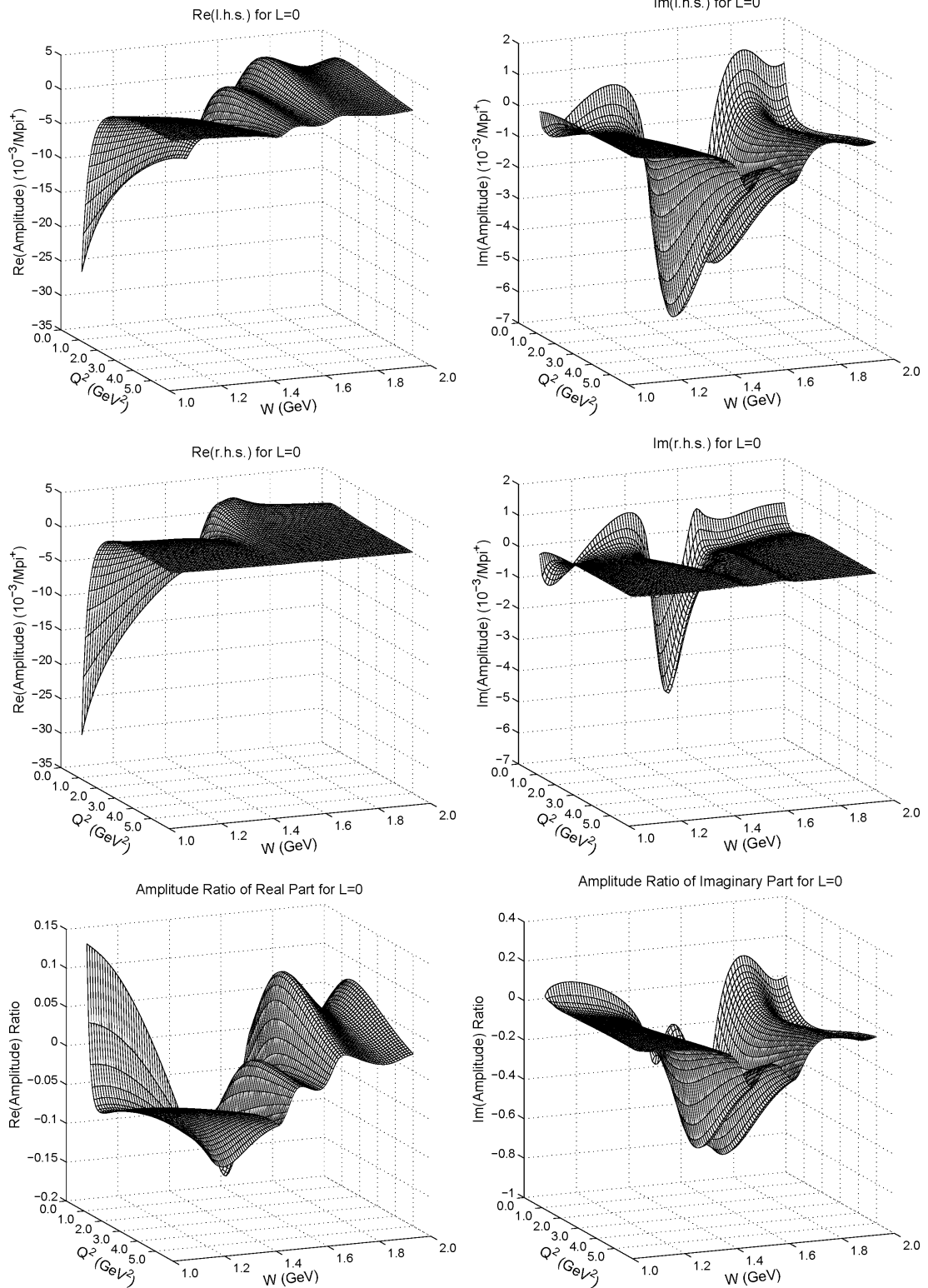
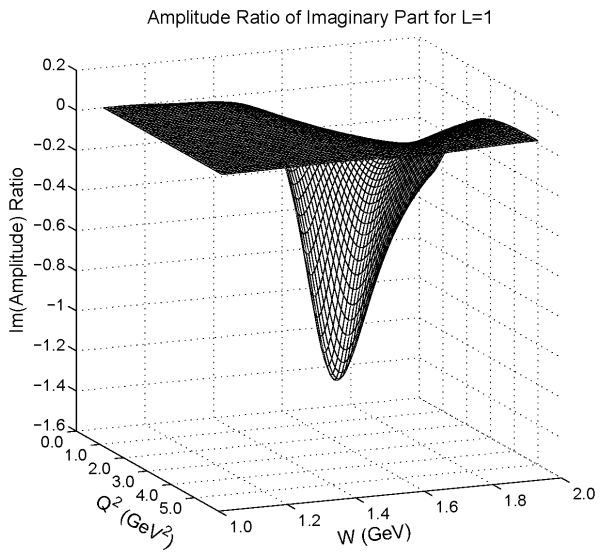
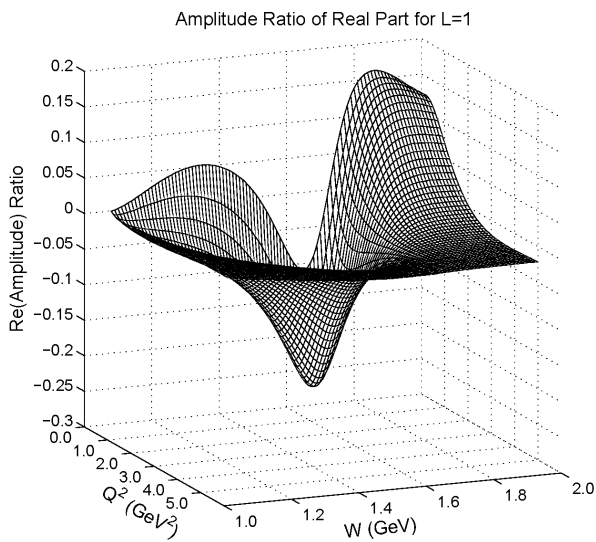
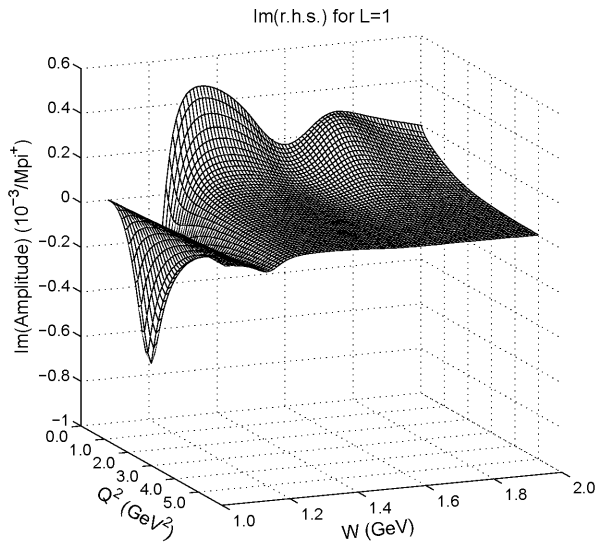
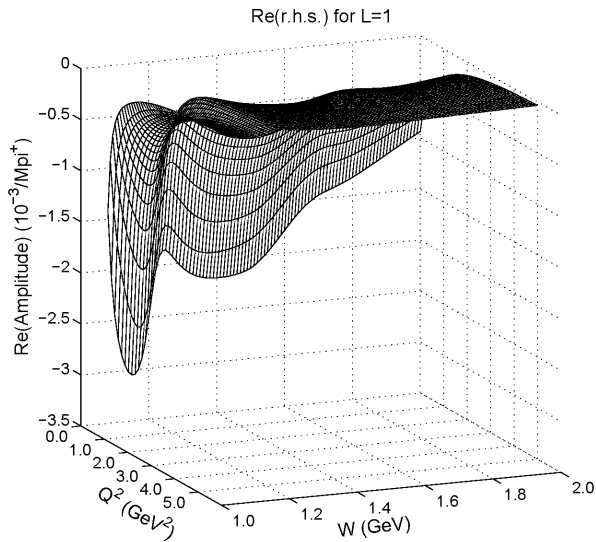
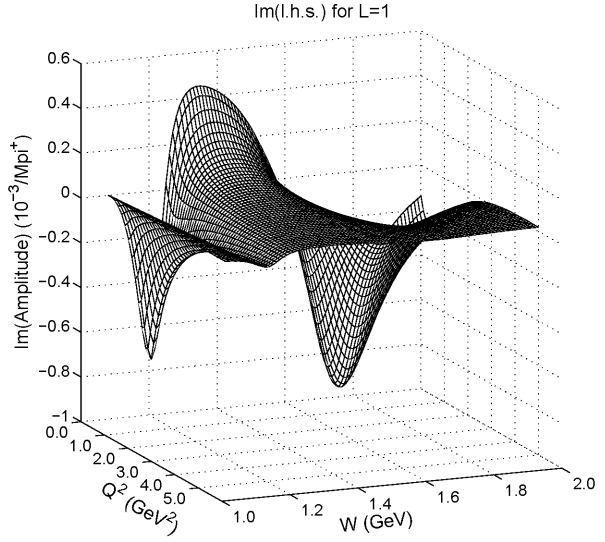
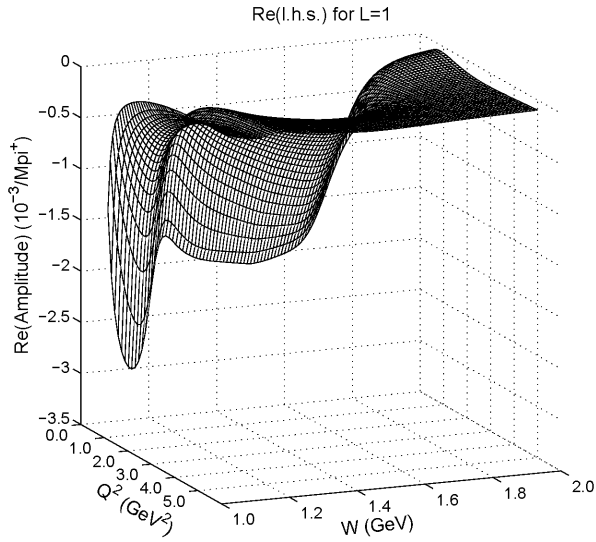
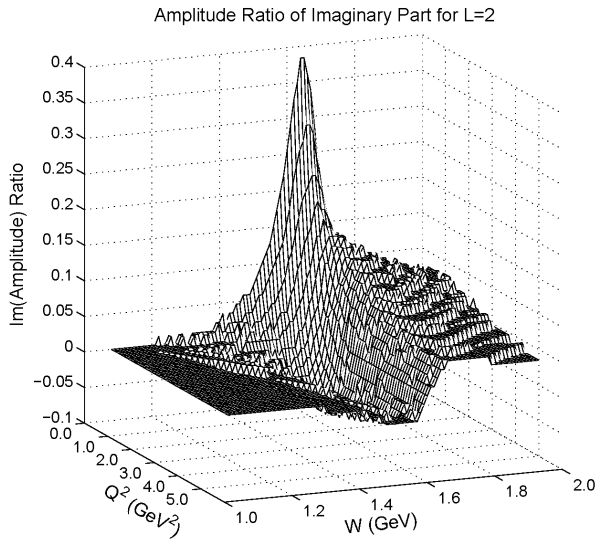
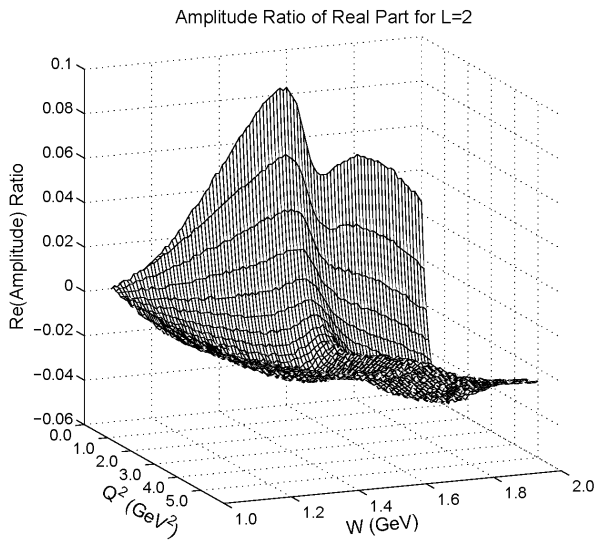
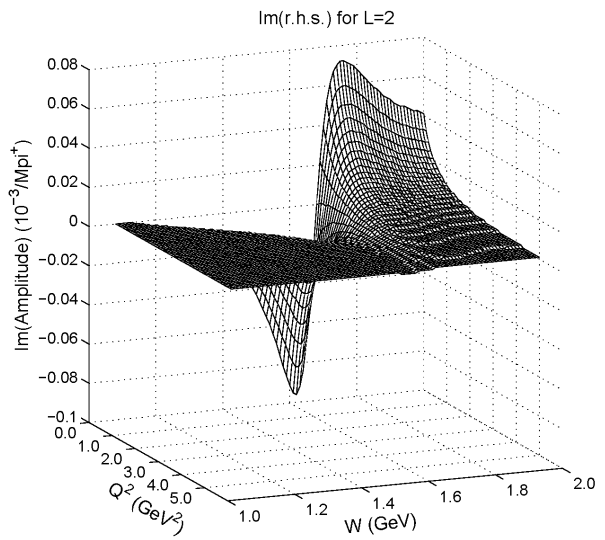
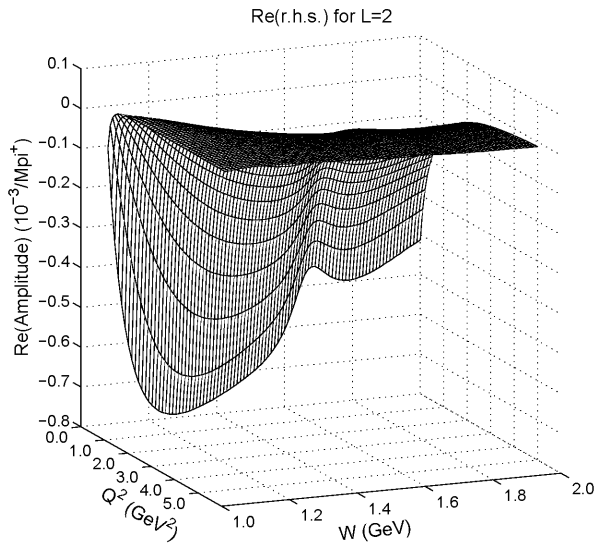
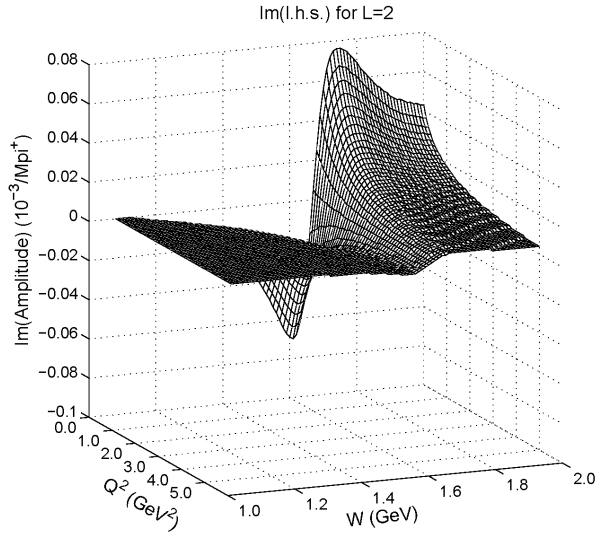
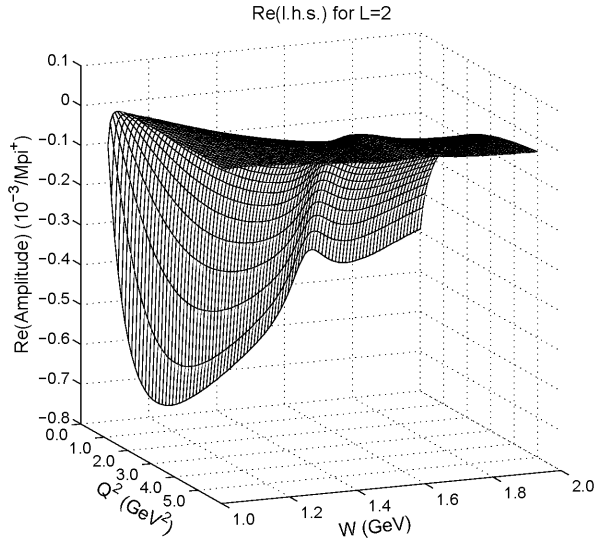
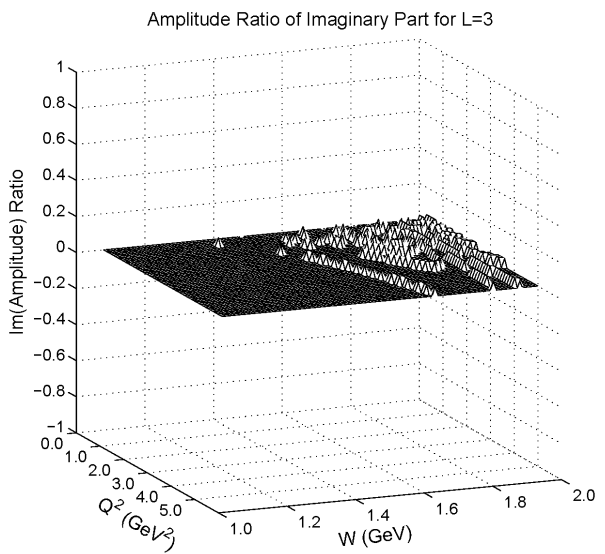
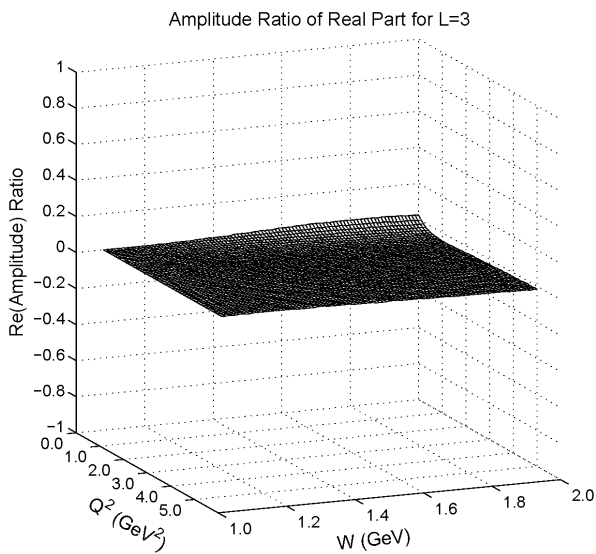
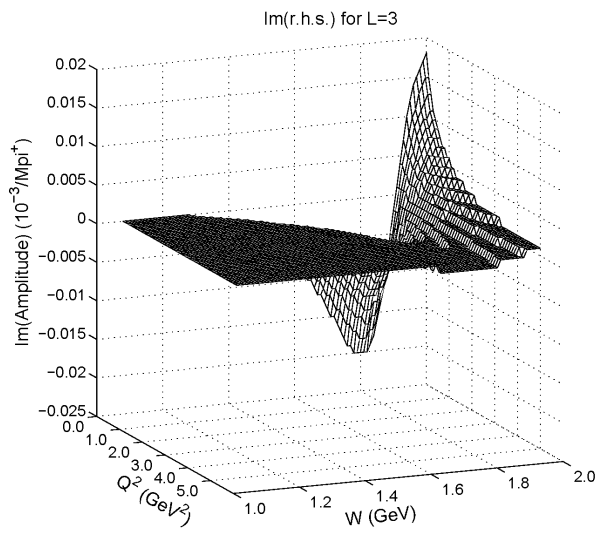
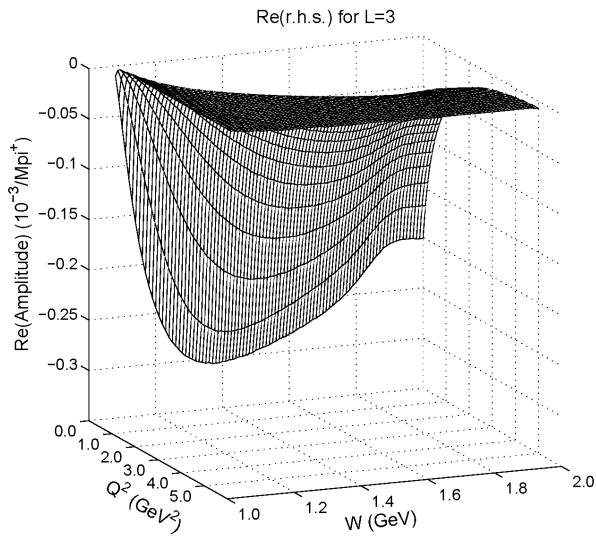
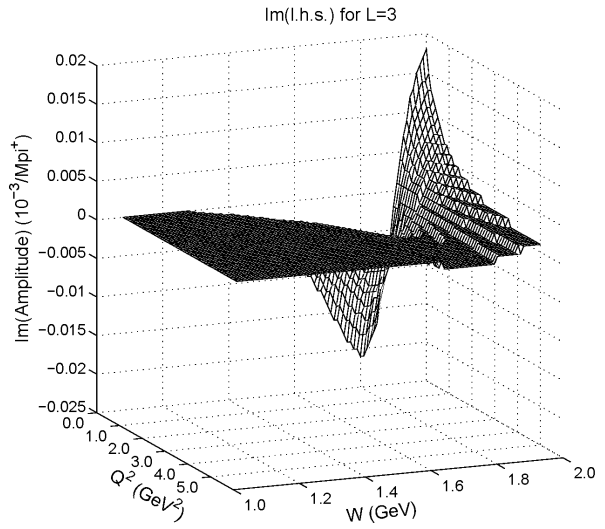
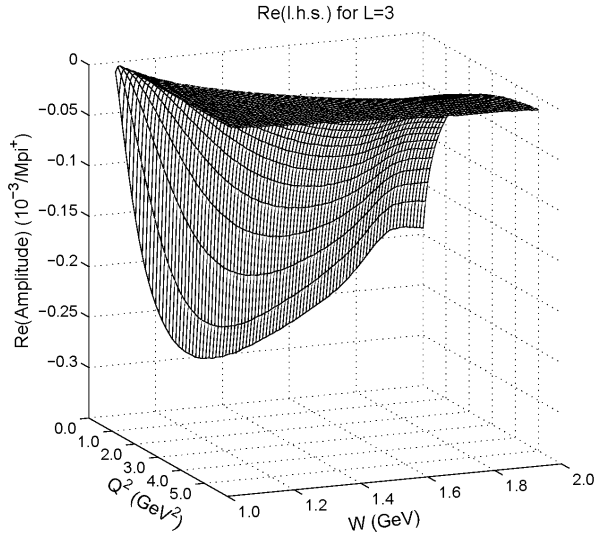


FIG. 3: Electric multipole data ($J = L + \frac{1}{2}$ amplitudes E_{L+}) from MAID 2007. The l.h.s., r.h.s., and ratio of relation (2.15) for $L \geq 0$ are presented in separate rows, with separate columns for the real and imaginary parts (except for the $L = 4$ and 5 imaginary parts, given as zero by MAID).









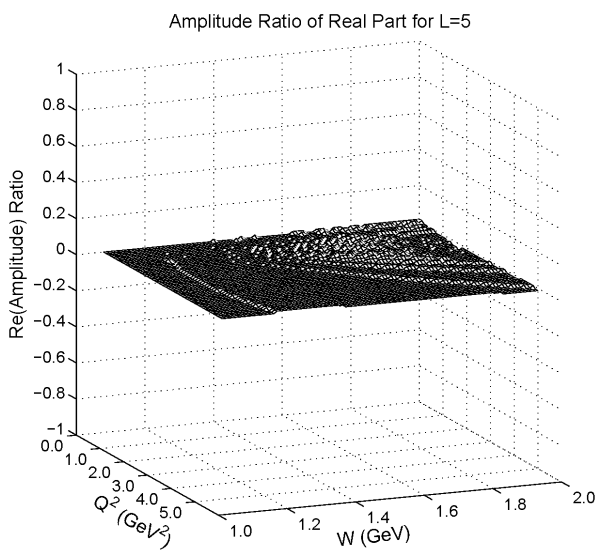
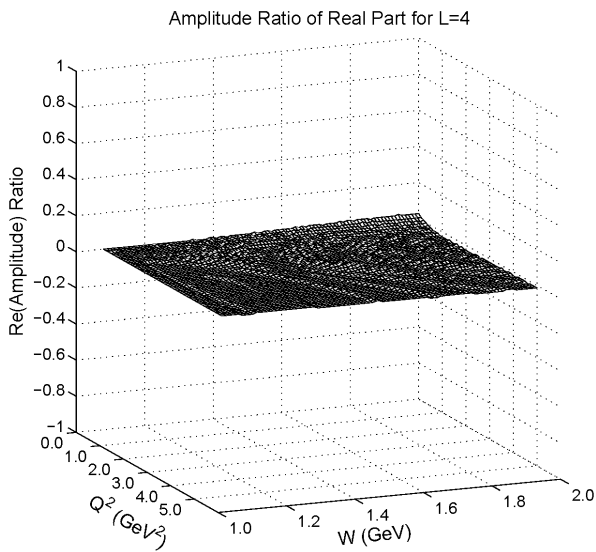
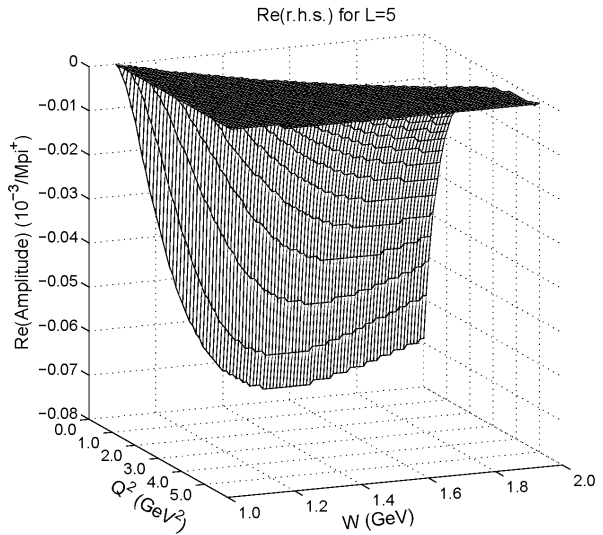
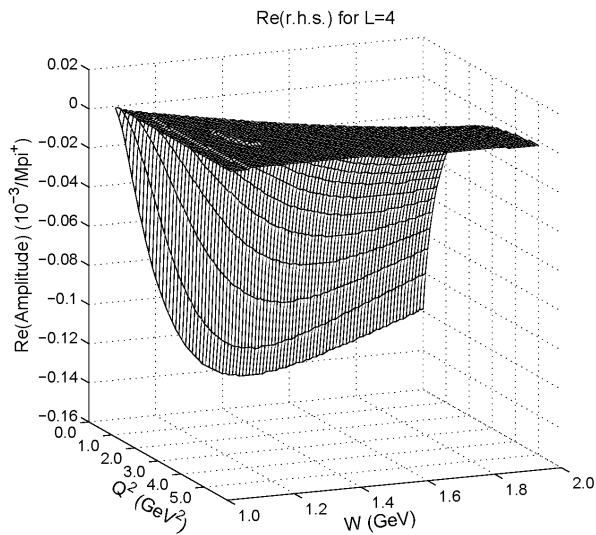
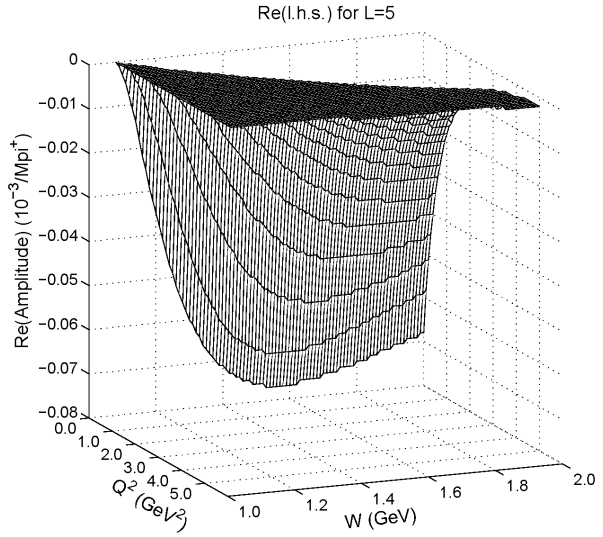
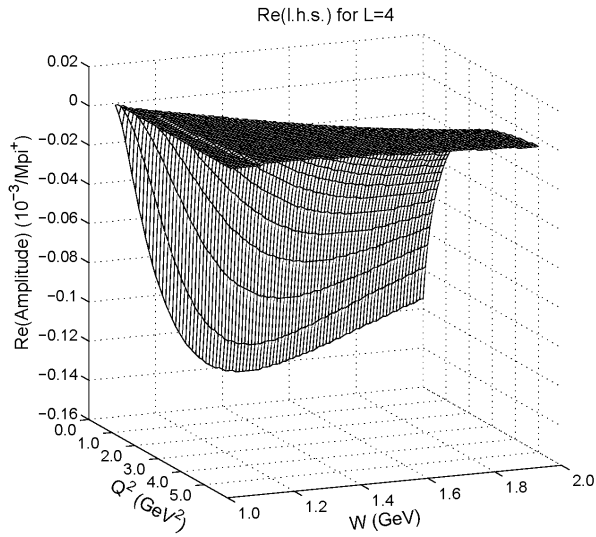
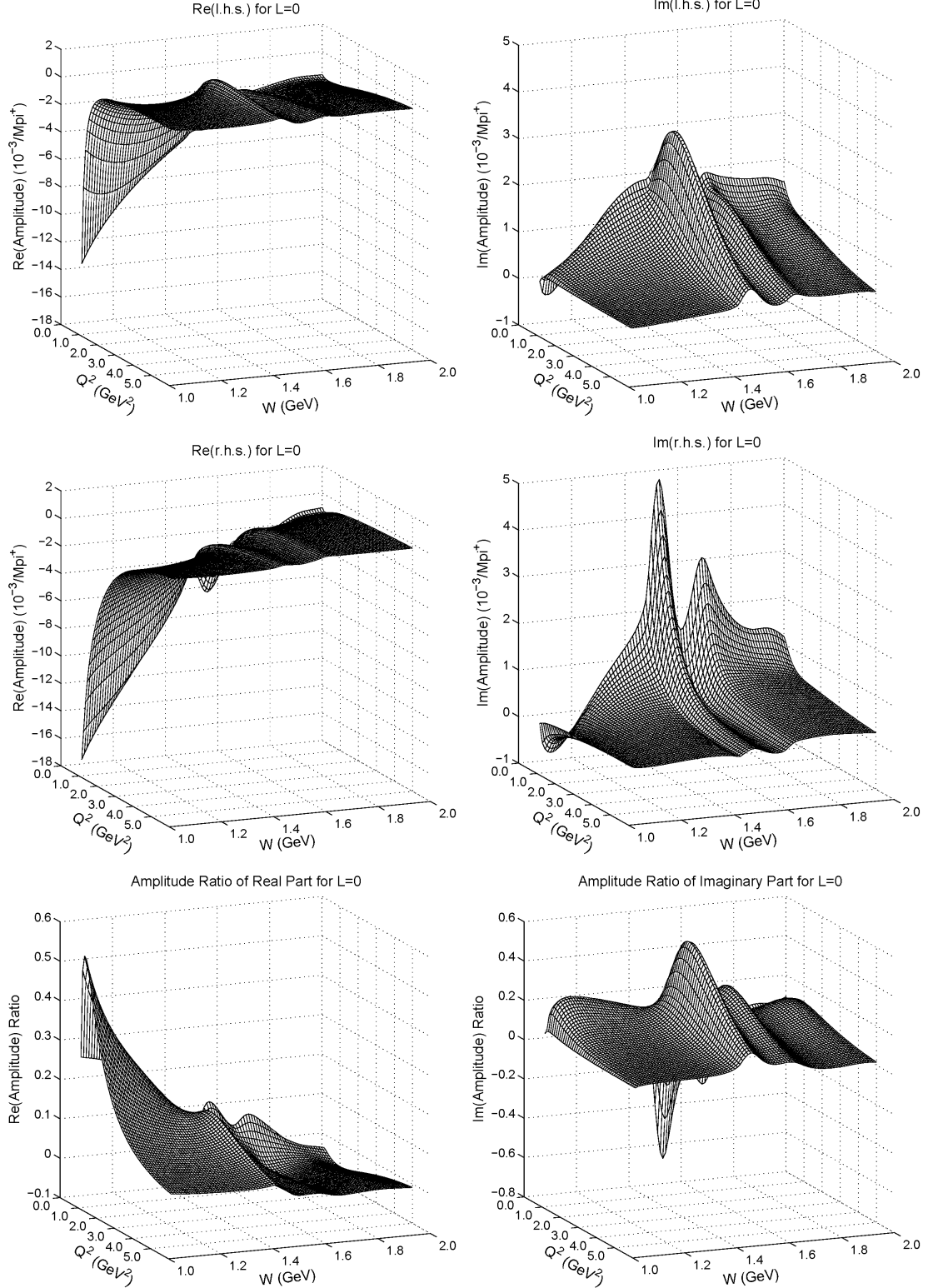
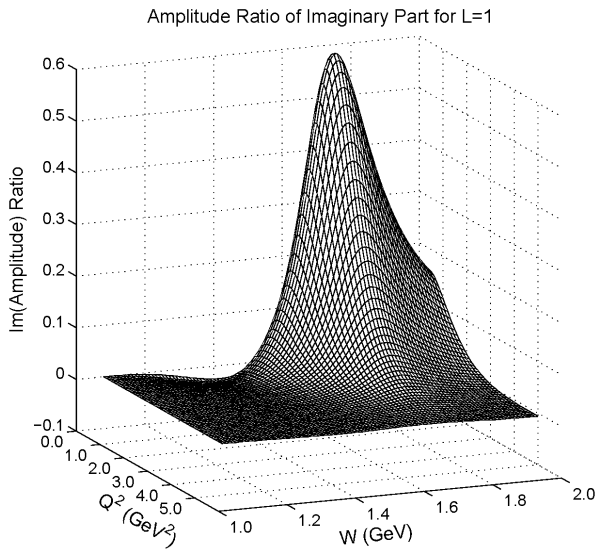
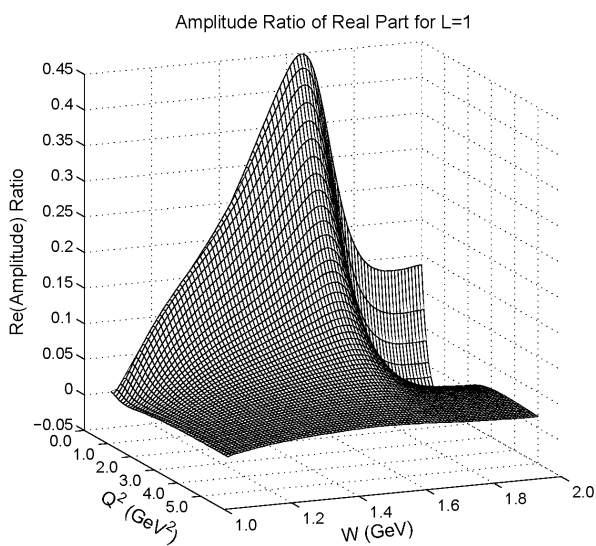
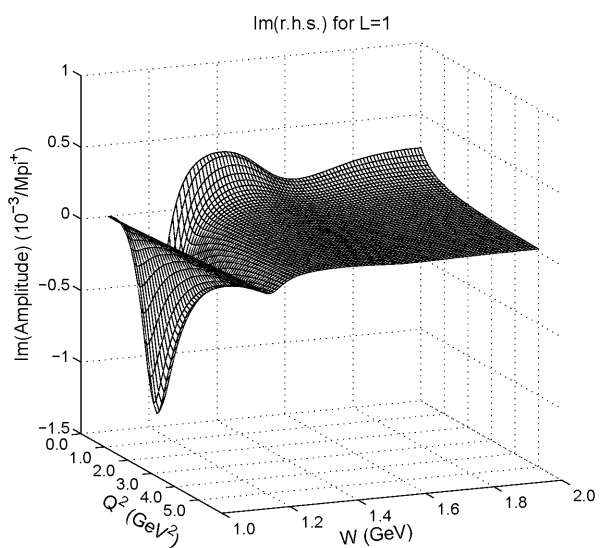
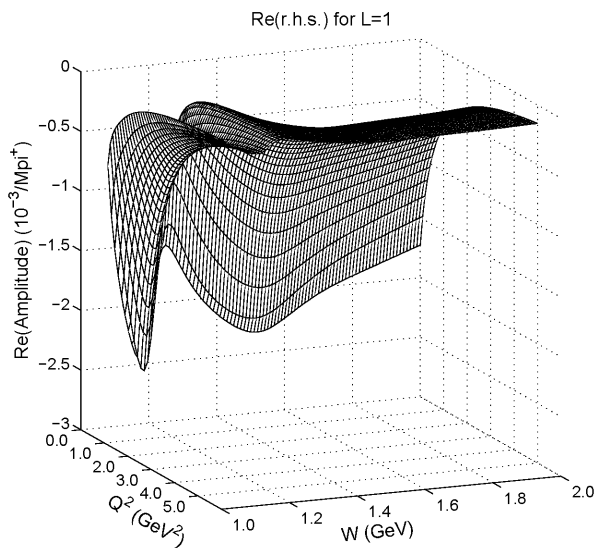
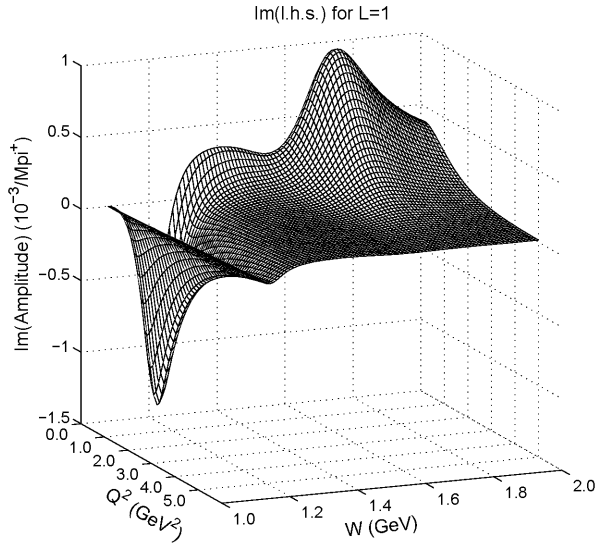
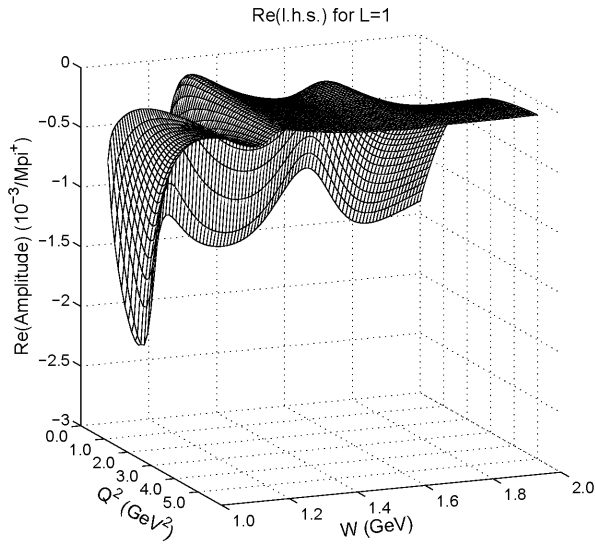
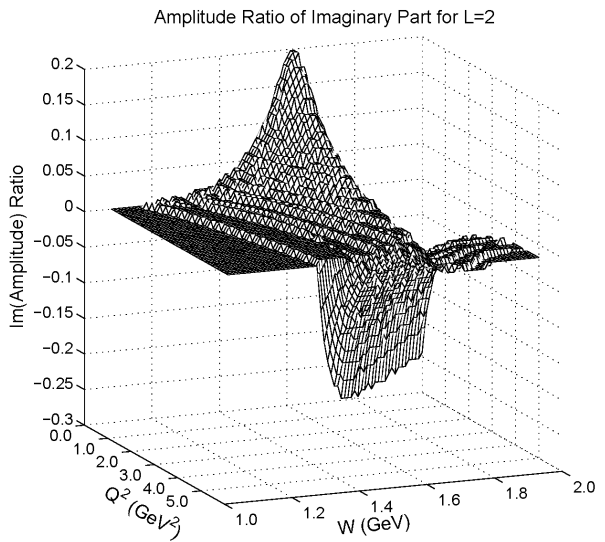
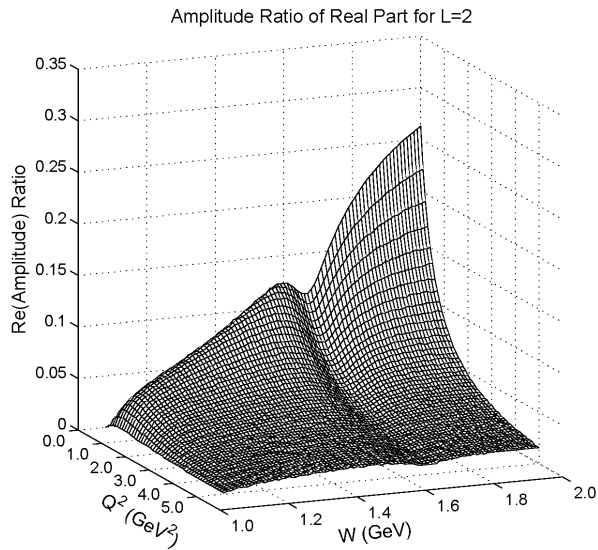
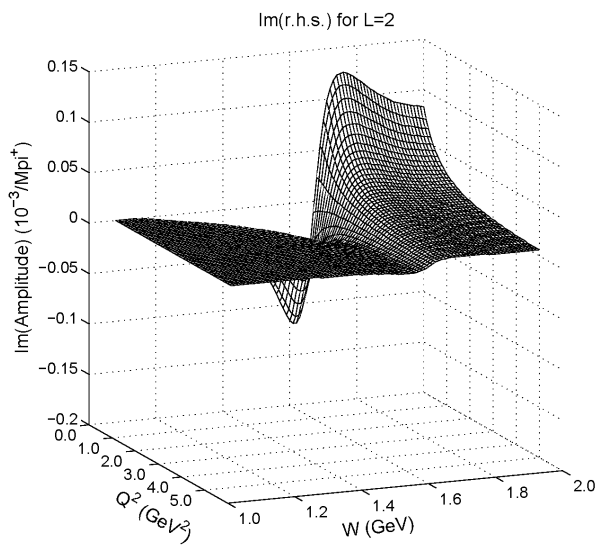
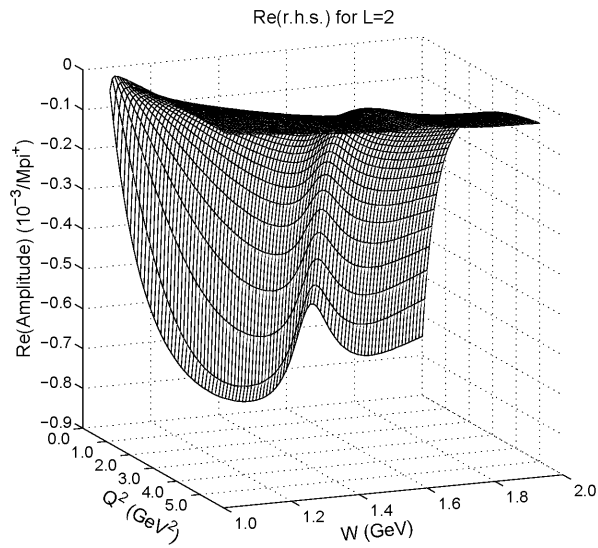
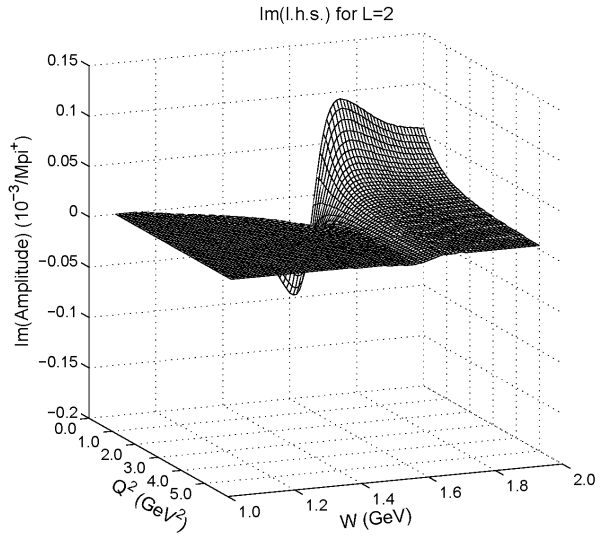
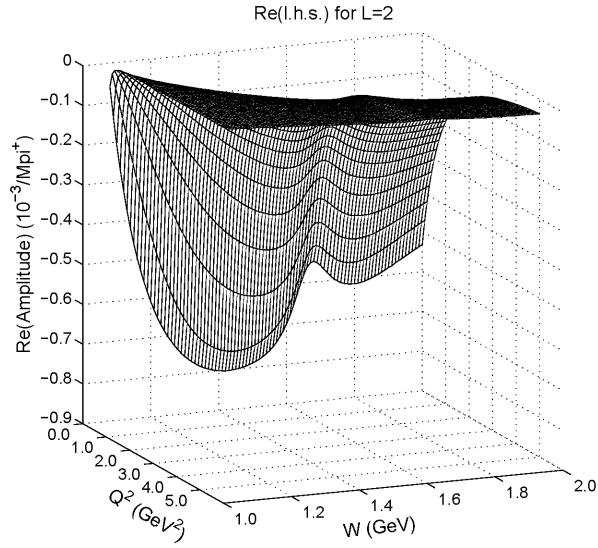
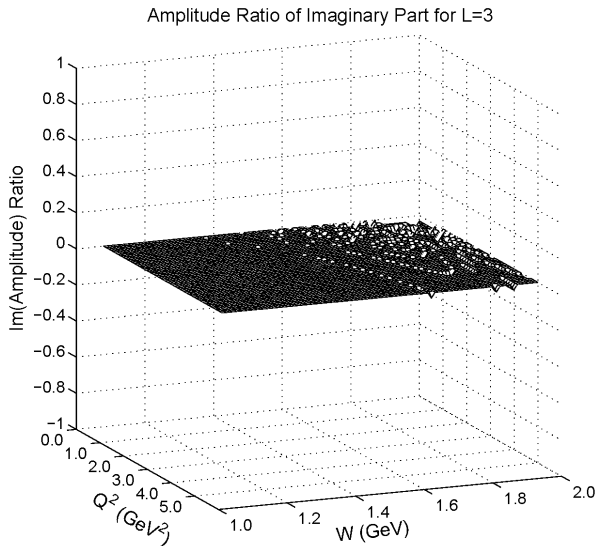
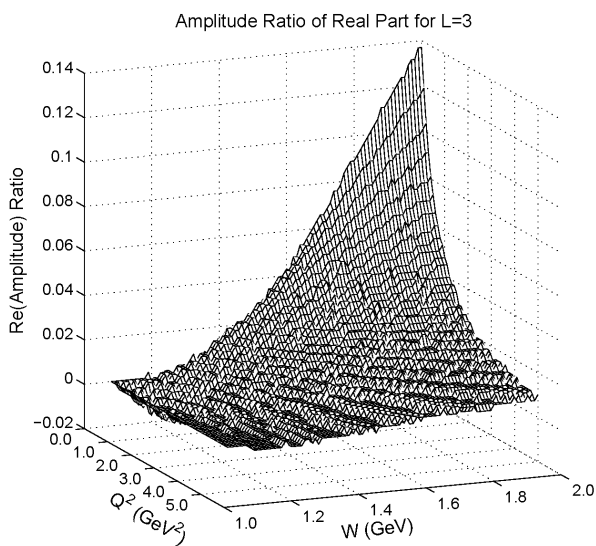
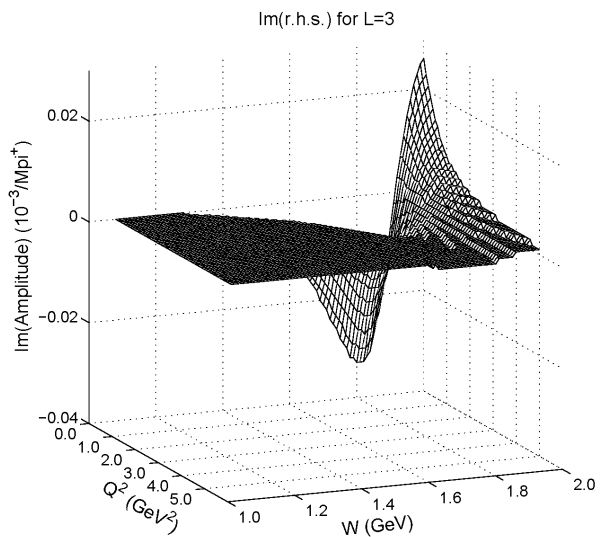
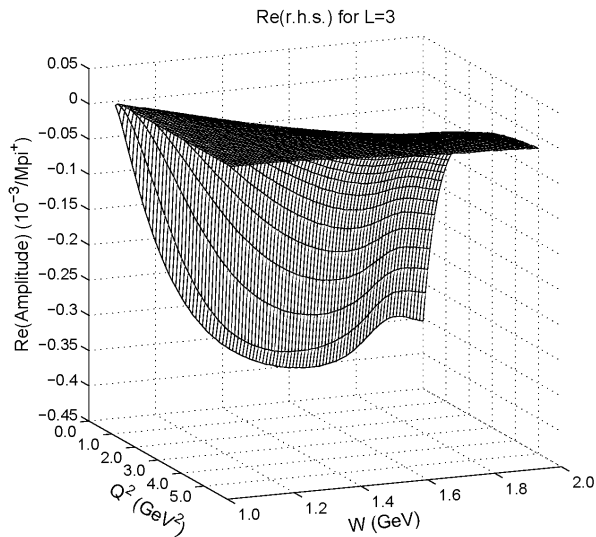
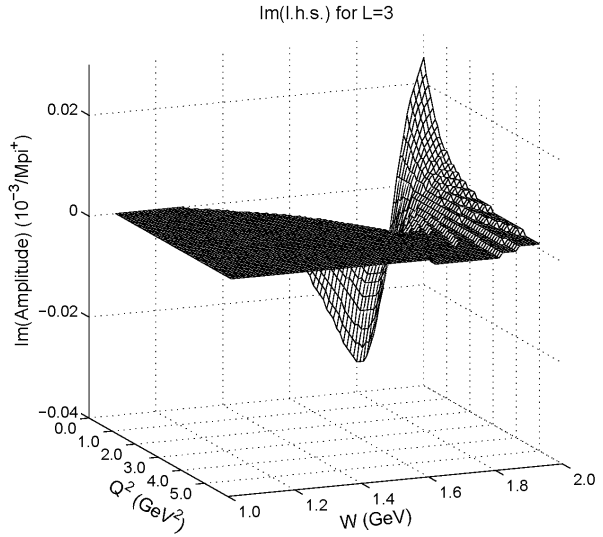
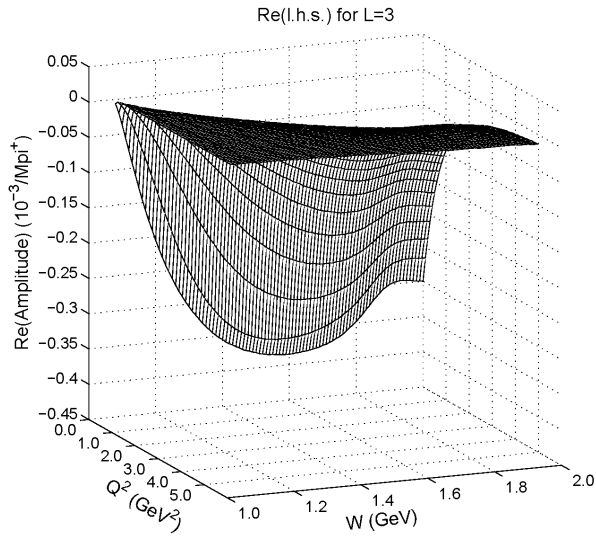


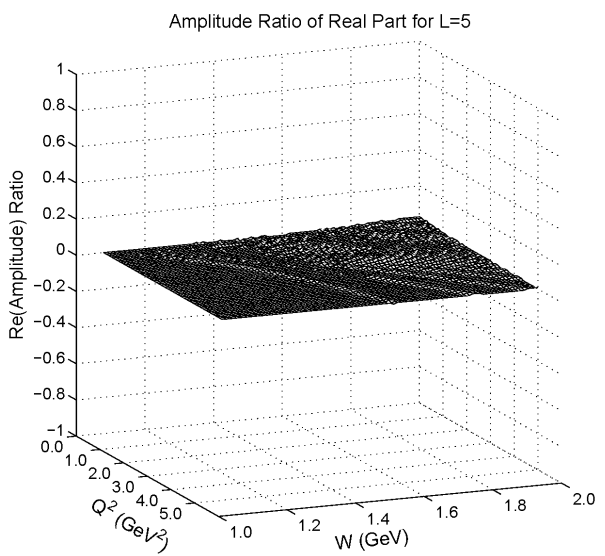
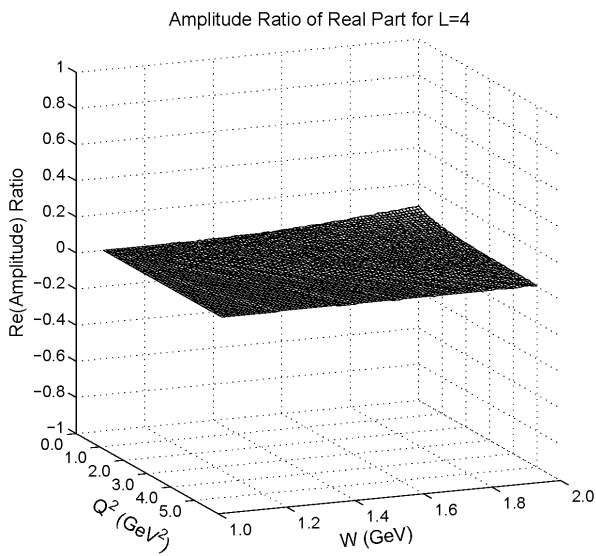
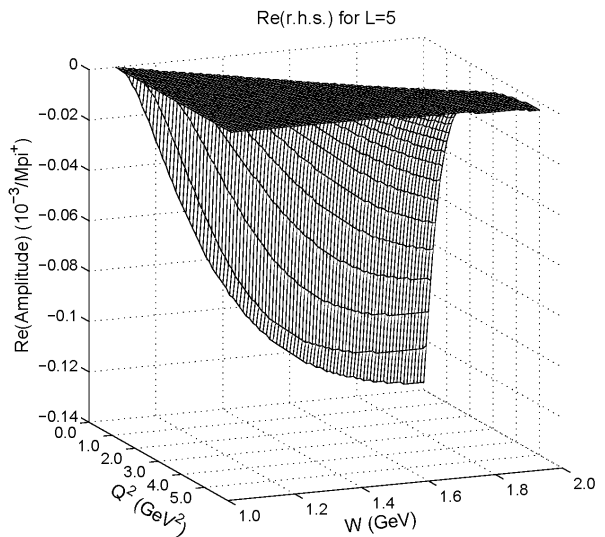
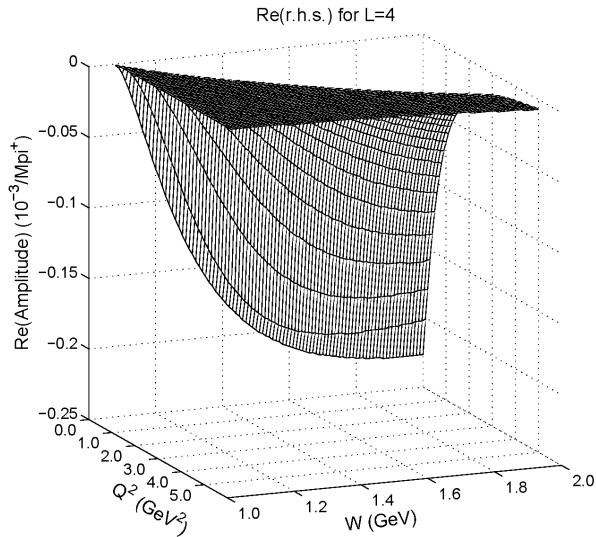
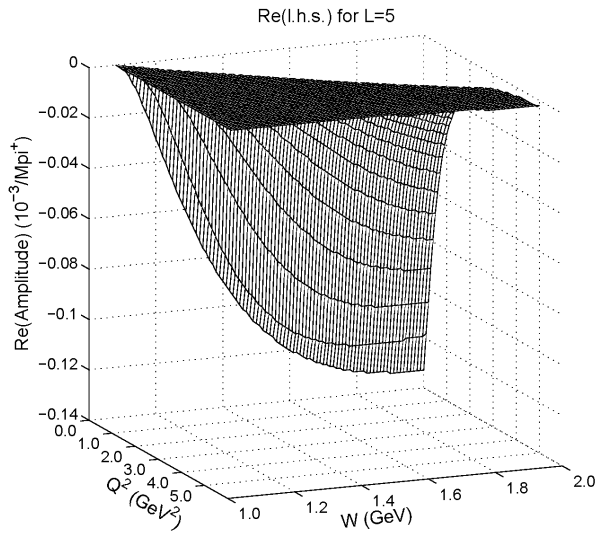
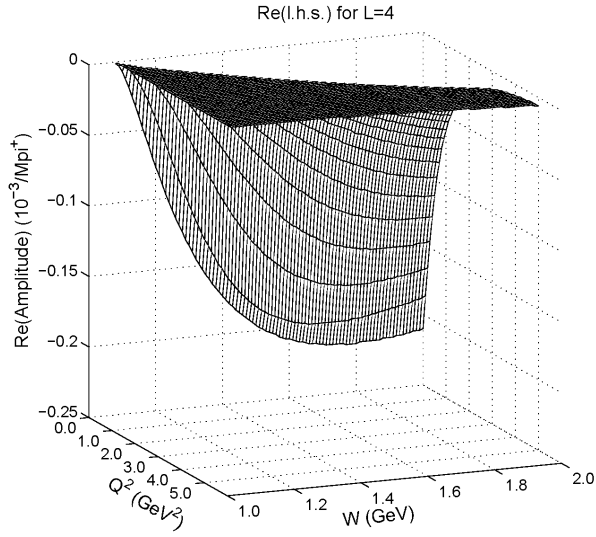
FIG. 4: Scalar multipole data ($J = L + \frac{1}{2}$ amplitudes S_{L+}) from MAID 2007. The l.h.s., r.h.s., and ratio of relation (2.15) for $L \geq 0$ are presented in separate rows, with separate columns for the real and imaginary parts (except for the $L = 4$ and 5 imaginary parts, given as zero by MAID).









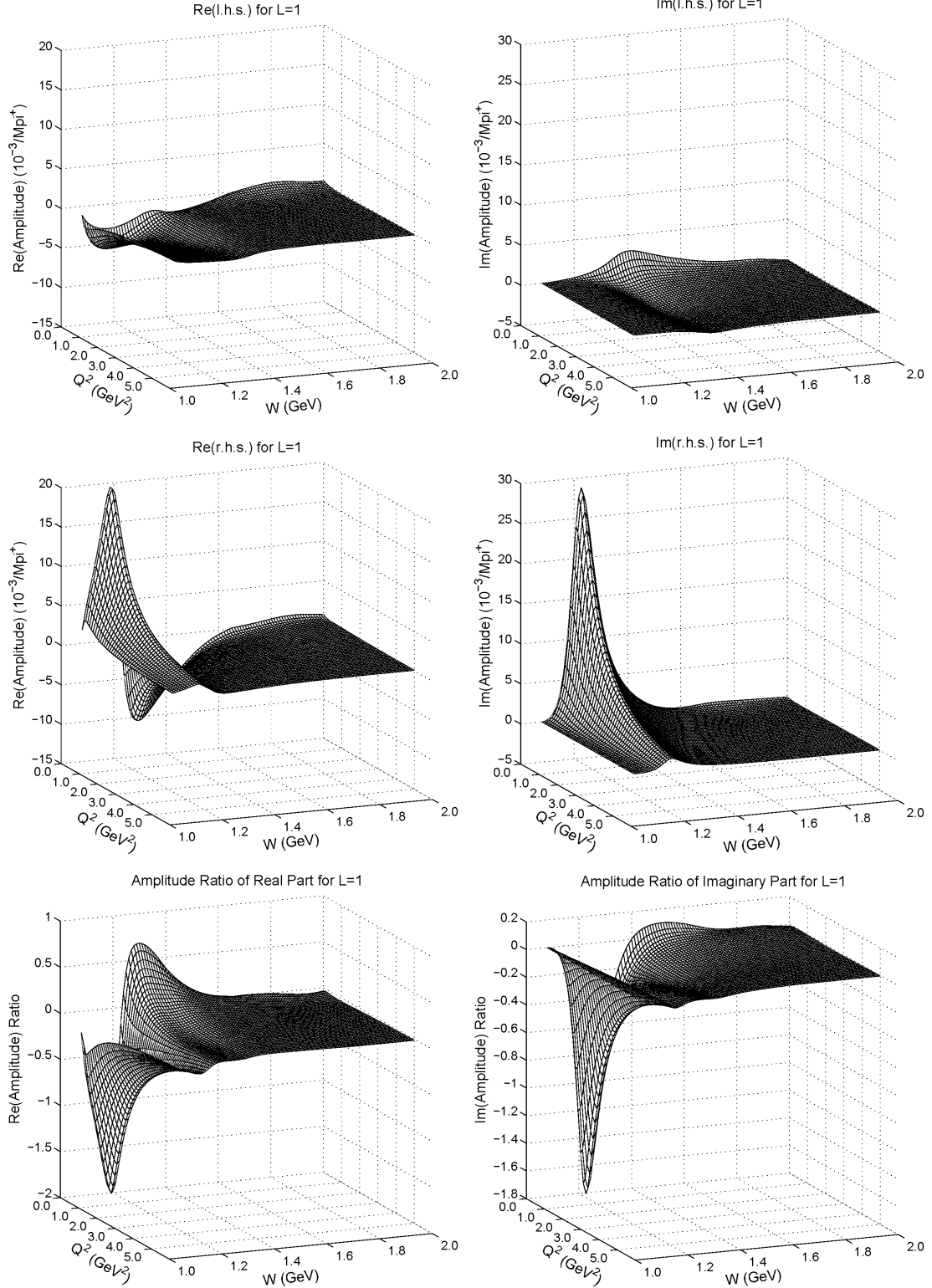


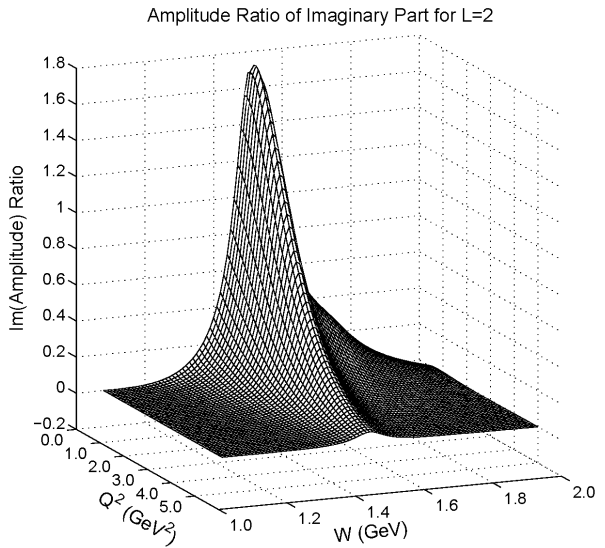
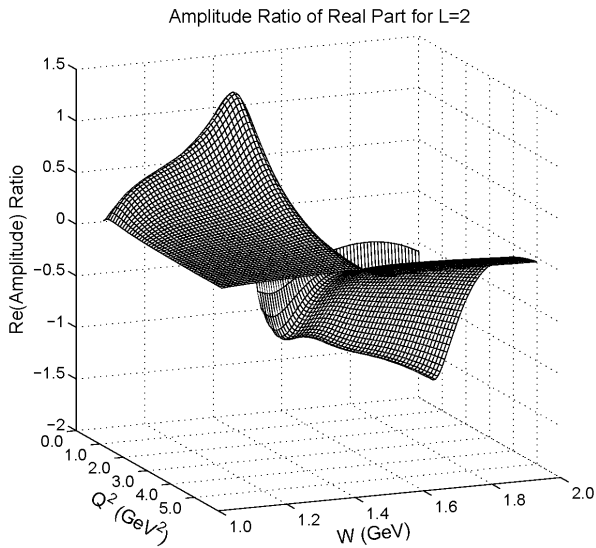
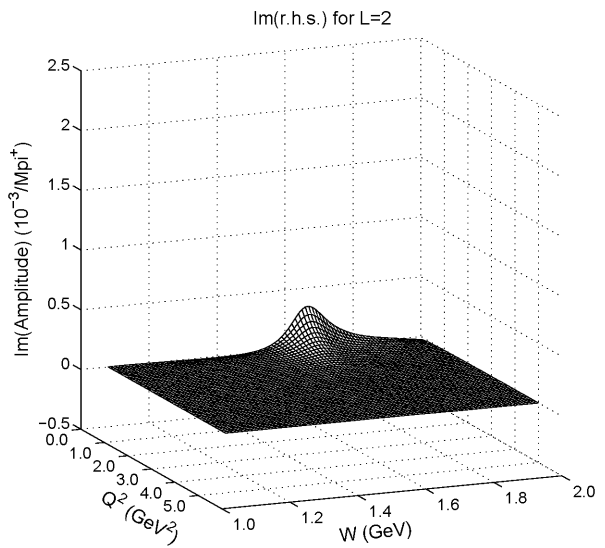
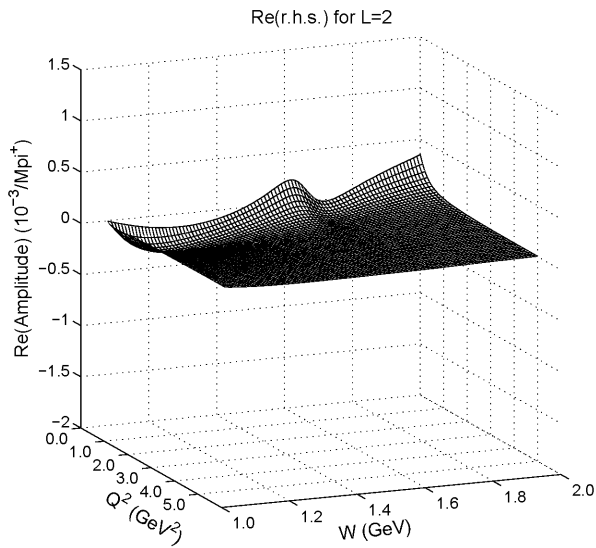
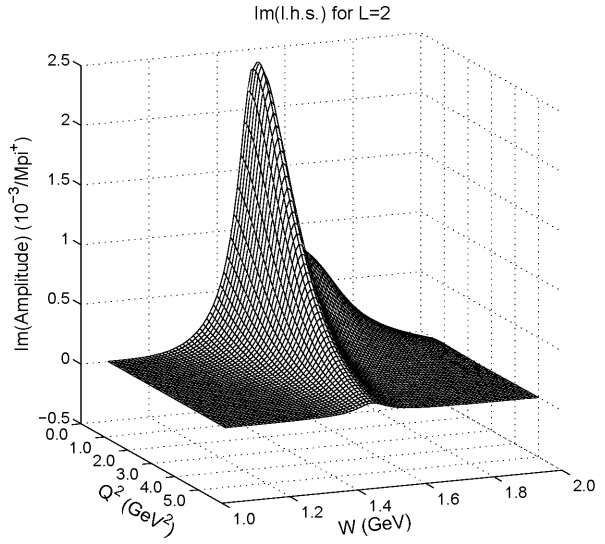
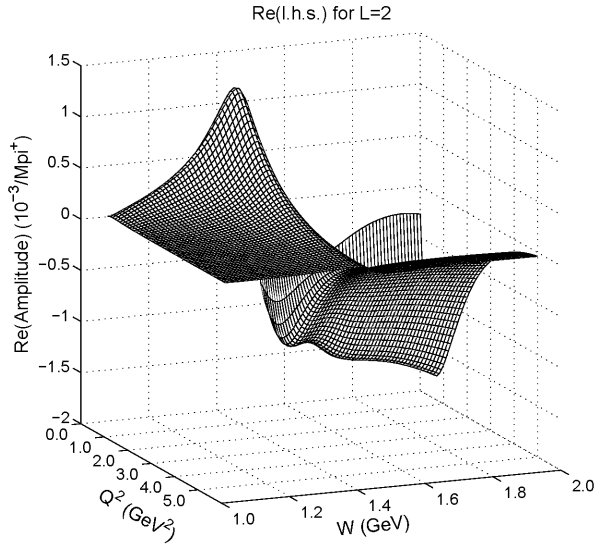
Acknowledgments

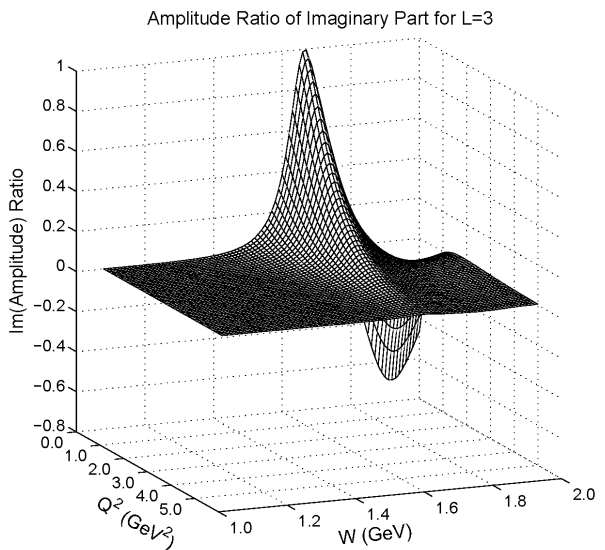
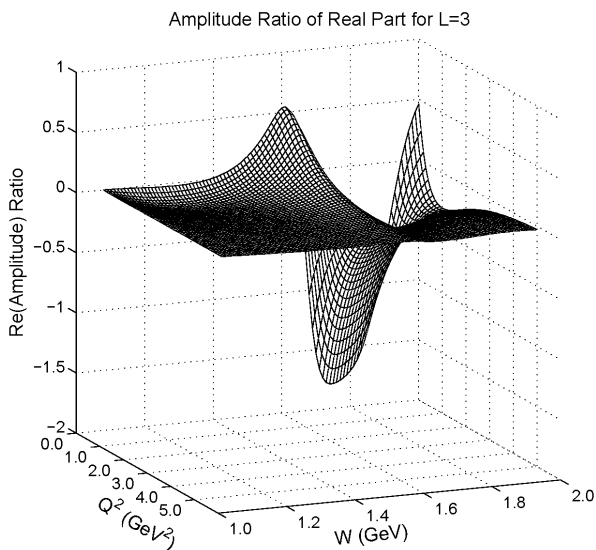
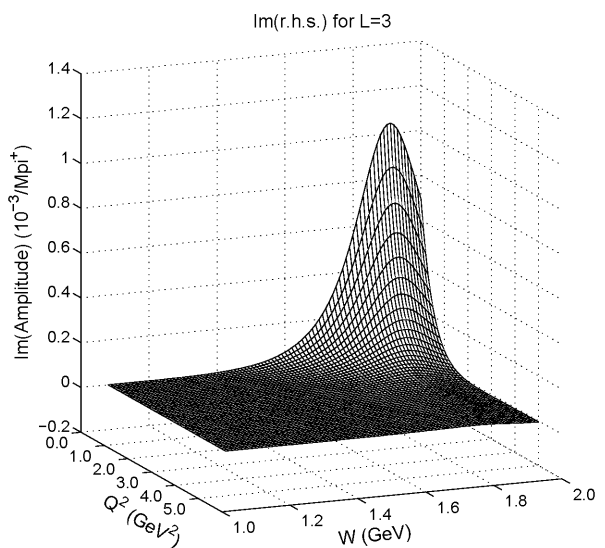
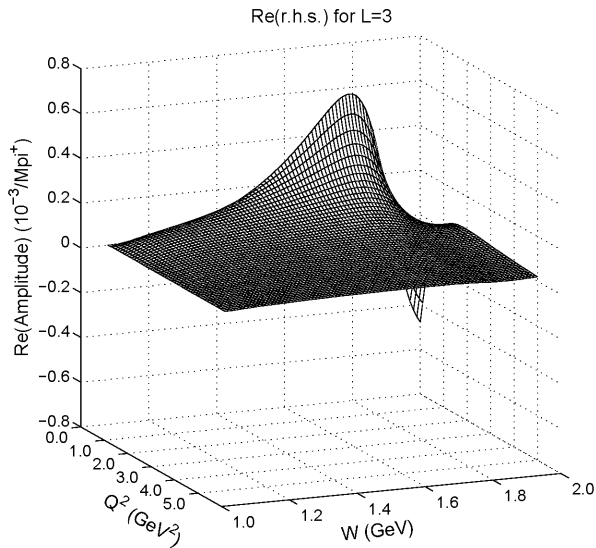
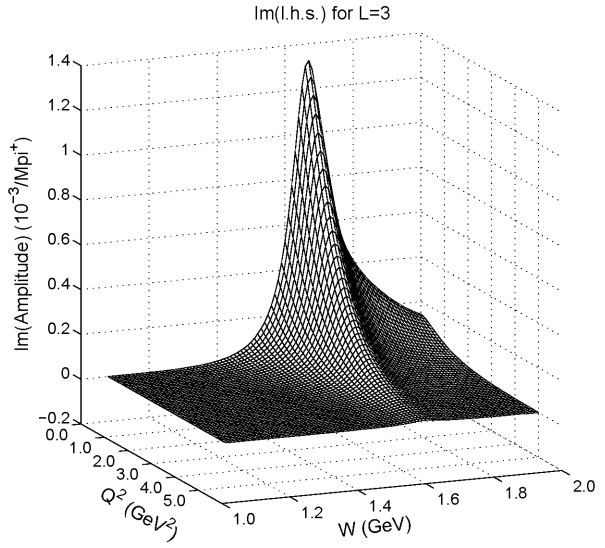
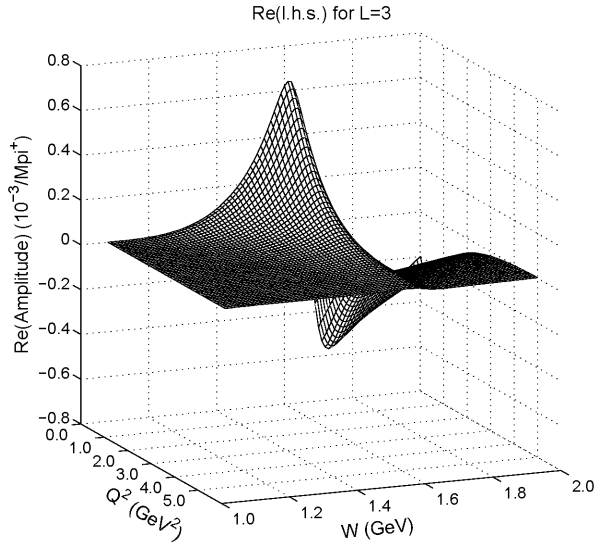
This work was supported by the NSF under Grant No. PHY-0757394.

- [1] G. 't Hooft, Nucl. Phys. B **72**, 461 (1974).
- [2] E. Witten, Nucl. Phys. B **160**, 57 (1979).
- [3] R.F. Dashen, E.E. Jenkins, and A.V. Manohar, Phys. Rev. D **49**, 4713 (1994) [Erratum-
ibid. D **51**, 2489 (1995)] [arXiv:hep-ph/9310379]; Phys. Rev. D **51**, 3697 (1995) [arXiv:hep-
ph/9411234]; J. Dai, R.F. Dashen, E.E. Jenkins, and A.V. Manohar, Phys. Rev. D **53**,
273 (1996) [arXiv:hep-ph/9506273]; E.E. Jenkins and A.V. Manohar, Phys. Lett. B **335**,
452 (1994) [arXiv:hep-ph/9405431]; E.E. Jenkins and R.F. Lebed, Phys. Rev. D **52**, 282
(1995) [arXiv:hep-ph/9502227]; E.E. Jenkins, Phys. Rev. D **54**, 4515 (1996) [arXiv:hep-
ph/9603449]; R. Flores-Mendieta, E.E. Jenkins, and A.V. Manohar, Phys. Rev. D **58**, 094028
(1998) [arXiv:hep-ph/9805416]; E.E. Jenkins, X.d. Ji, and A.V. Manohar, Phys. Rev. Lett.
89, 242001 (2002) [arXiv:hep-ph/0207092]; M.A. Luty and J. March-Russell, Nucl. Phys.
B **426**, 71 (1994) [arXiv:hep-ph/9310369]; M.A. Luty, J. March-Russell, and M.J. White,
Phys. Rev. D **51**, 2332 (1995) [arXiv:hep-ph/9405272]; C. Carone, H. Georgi, and S. Osof-
sky, Phys. Lett. B **322**, 227 (1994) [arXiv:hep-ph/9310365]; C.D. Carone, H. Georgi, L. Ka-
plan, and D. Morin, Phys. Rev. D **50**, 5793 (1994) [arXiv:hep-ph/9406227]; D. Pirjol and
T.M. Yan, Phys. Rev. D **56**, 5483 (1997) [arXiv:hep-ph/9701291]; Phys. Rev. D **57**, 5434
(1998) [arXiv:hep-ph/9711201]; C.E. Carlson, C.D. Carone, J.L. Goity, and R.F. Lebed, Phys.
Lett. B **438**, 327 (1998) [arXiv:hep-ph/9807334]; Phys. Rev. D **59**, 114008 (1999) [arXiv:hep-
ph/9812440]; C.E. Carlson and C.D. Carone, Phys. Lett. B **484**, 260 (2000) [arXiv:hep-
ph/0005144]; C.L. Schat, J.L. Goity, and N.N. Scoccola, Phys. Rev. Lett. **88**, 102002 (2002)
[arXiv:hep-ph/0111082]; J.L. Goity, C.L. Schat, and N.N. Scoccola, Phys. Rev. D **66**, 114014
(2002) [arXiv:hep-ph/0209174]; D. Pirjol and C. Schat, Phys. Rev. D **67**, 096009 (2003)
[arXiv:hep-ph/0301187]; Phys. Rev. D **71**, 036004 (2005) [arXiv:hep-ph/0408293]; J.L. Goity,
C. Schat, and N.N. Scoccola, Phys. Lett. B **564**, 83 (2003) [arXiv:hep-ph/0304167]; J.L. Goity,
C. Schat and N. Scoccola, Phys. Rev. D **71**, 034016 (2005) [arXiv:hep-ph/0411092]; J.L. Goity
and N.N. Scoccola, Phys. Rev. D **72**, 034024 (2005) [arXiv:hep-ph/0504101]; R.F. Lebed

FIG. 5: Magnetic multipole (π^0) data from MAID 2007. The l.h.s. (M_{L-}), r.h.s. (M_{L+}), and ratio of relation (2.17) for $L \geq 1$ are presented in separate rows, with separate columns for the real and imaginary parts (except for the $L = 4$ and 5 imaginary parts, given as zero by MAID).







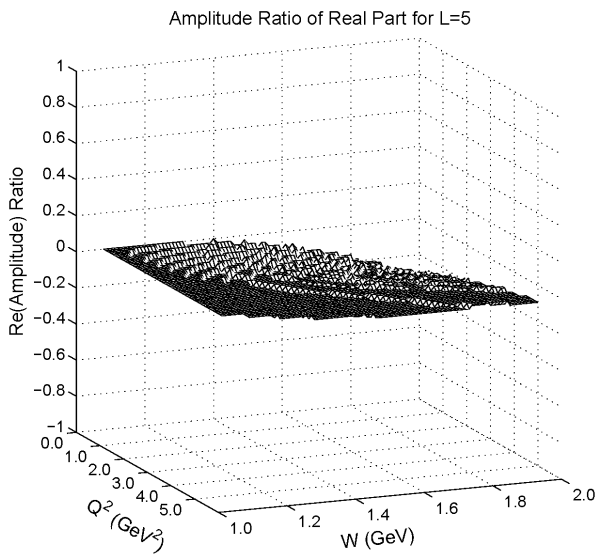
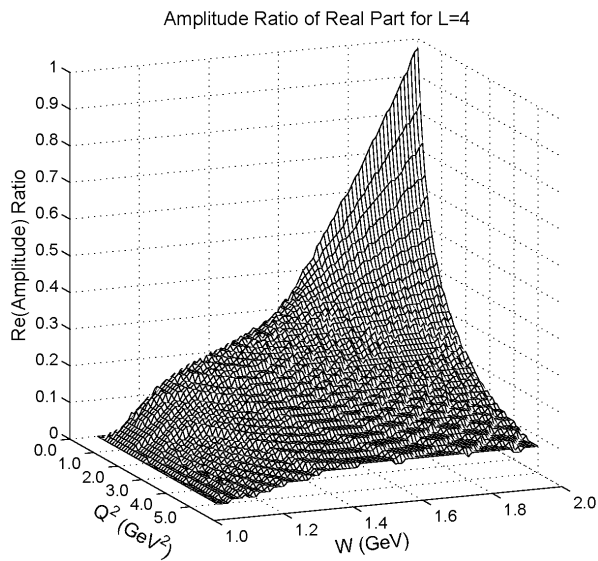
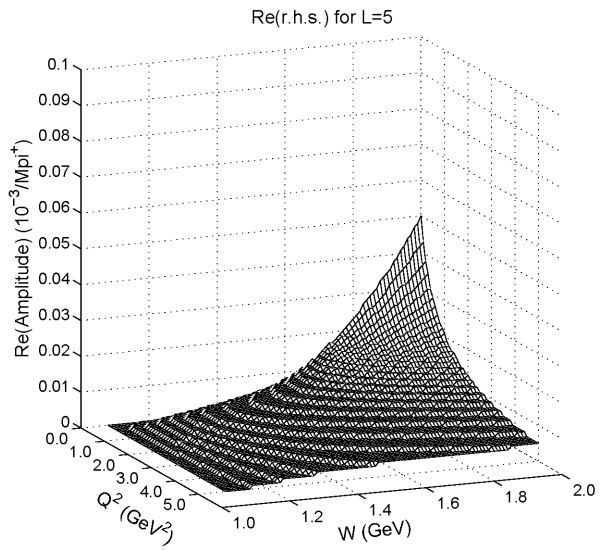
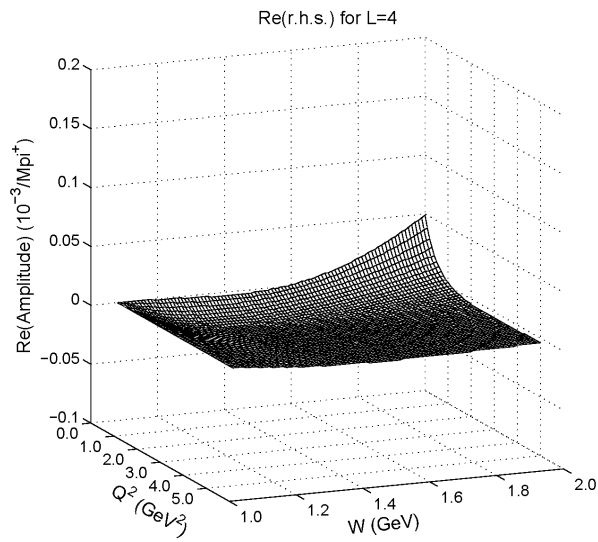
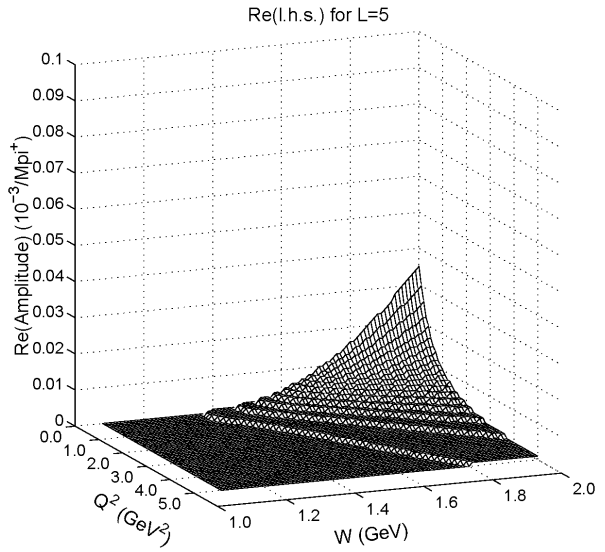
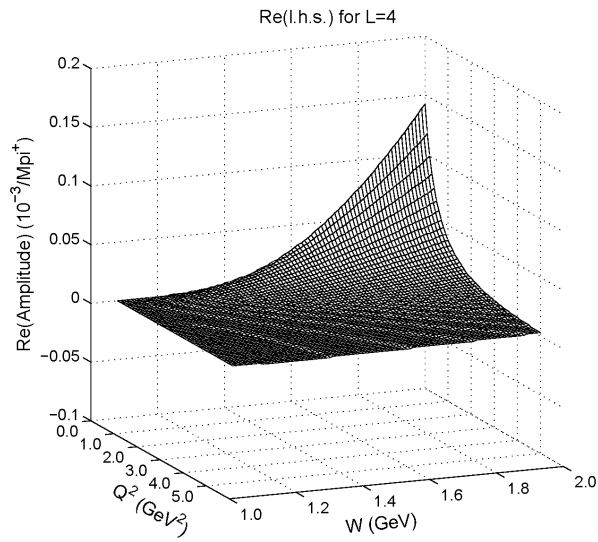
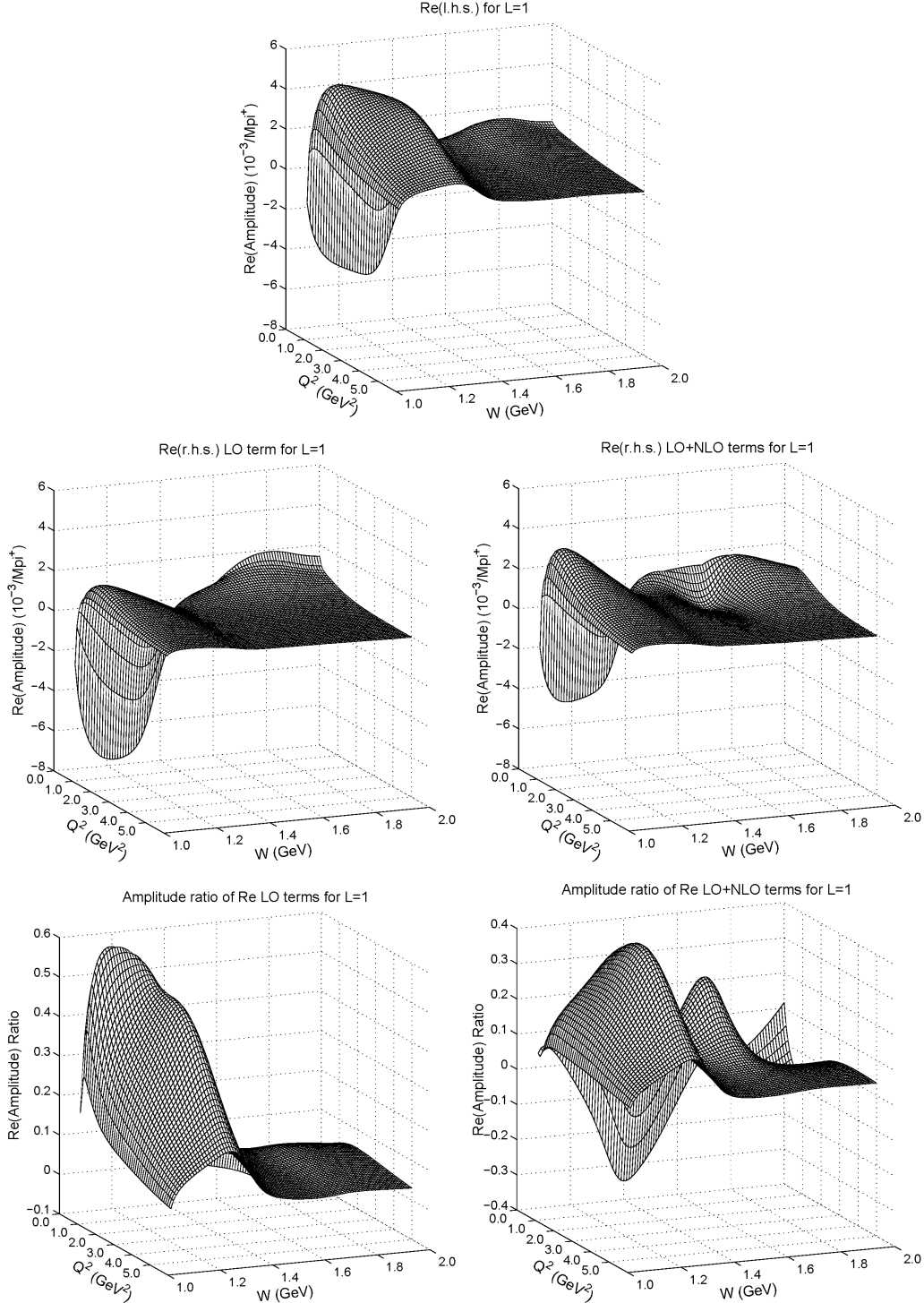
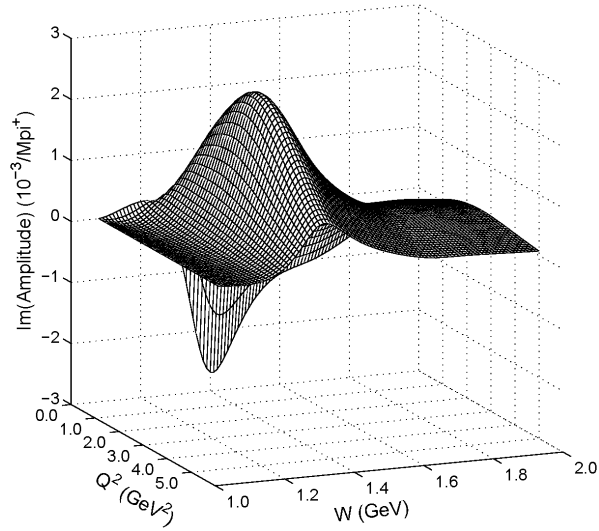


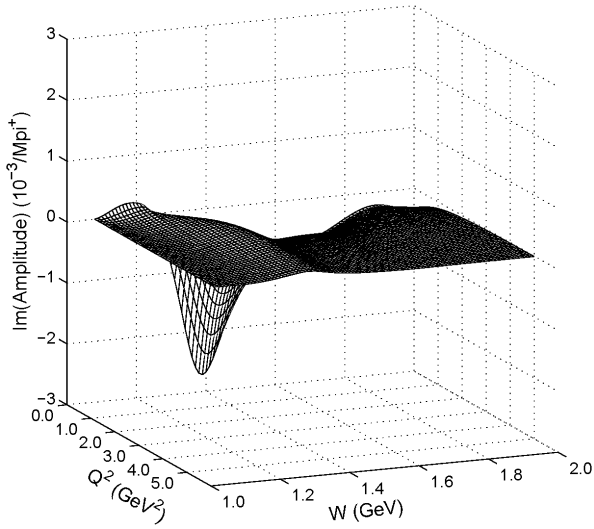
FIG. 6: Magnetic multipole (π^\pm) data from MAID 2007. Each $L \geq 1$ fills a separate page for real and imaginary parts of amplitudes (except for $L = 4$ and 5 imaginary parts, given as zero by MAID). The l.h.s. of relation (2.18) [or (2.19)] is indicated in the first row, while the LO term [first r.h.s. of relation (2.18)] and its ratio are presented in the left column, and the (LO+NLO) combination [r.h.s. of relation (2.19)] and its ratio are presented in the right column.



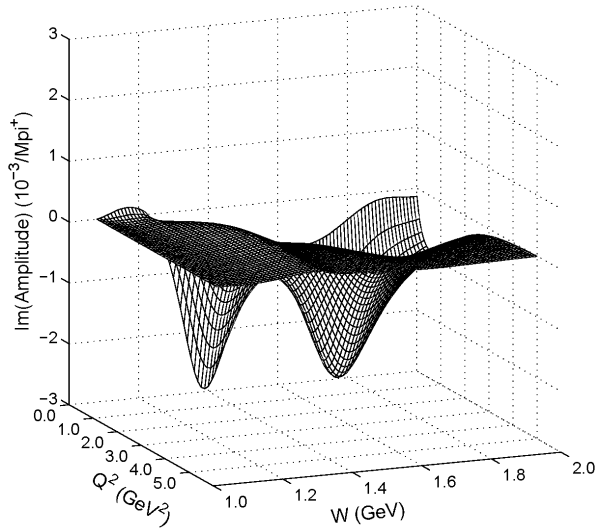
Im(l.h.s.) for L=1



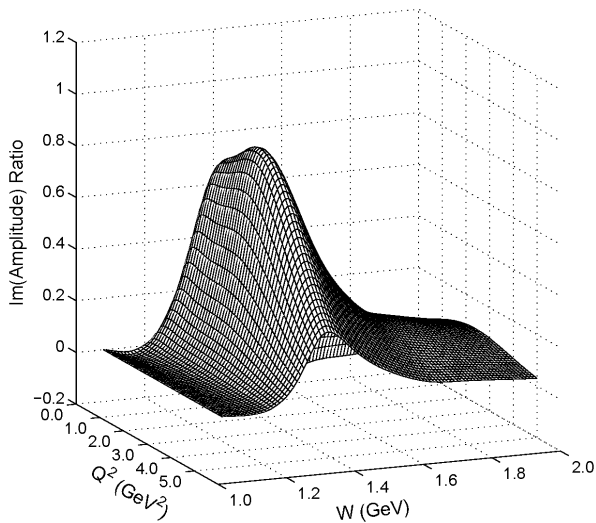
Im(r.h.s.) LO term for L=1



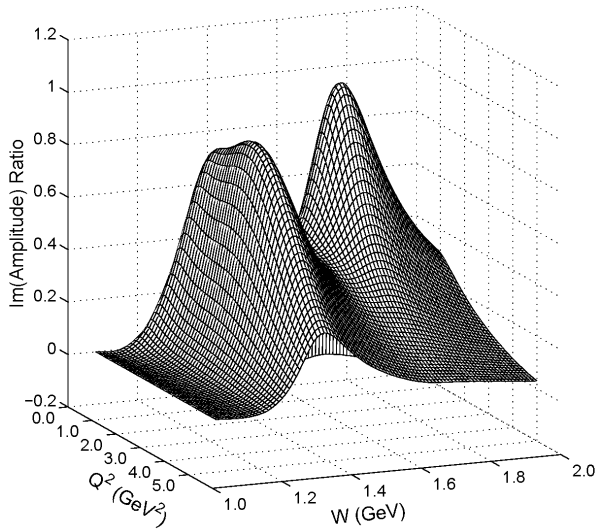
Im(r.h.s.) LO+NLO terms for L=1



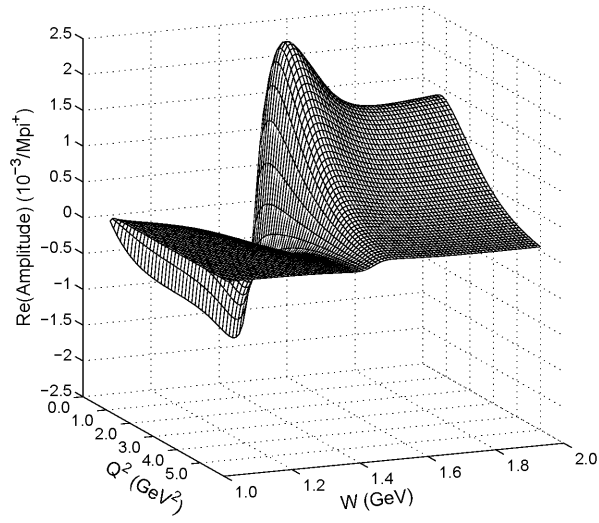
Amplitude ratio of Im LO terms for L=1



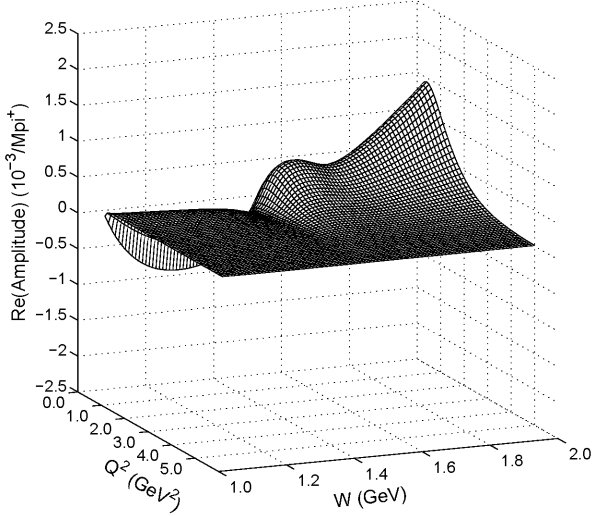
Amplitude ratio of Im LO+NLO terms for L=1



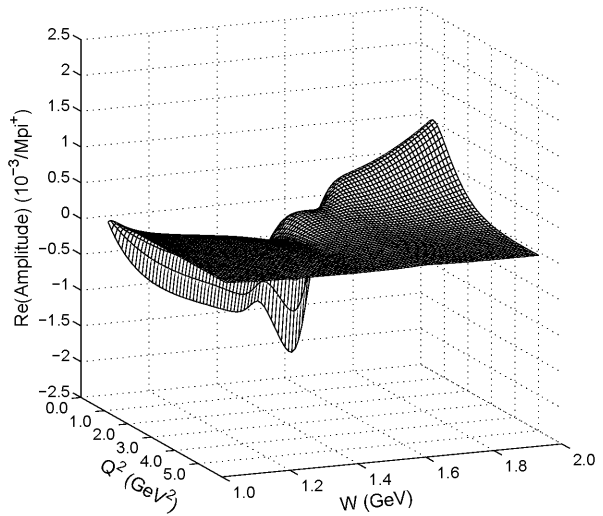
Re(l.h.s.) for L=2



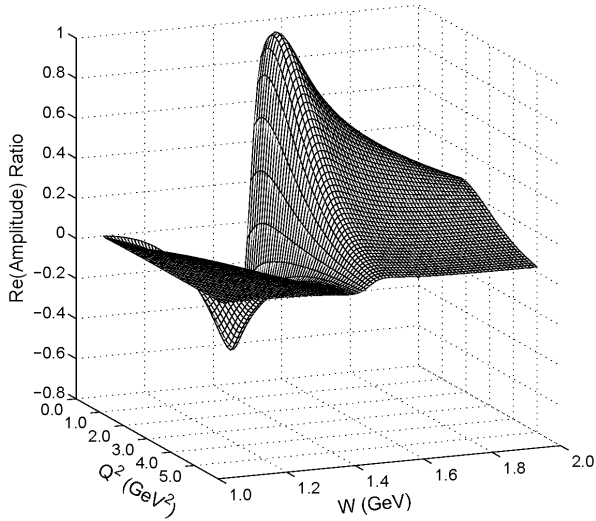
Re(r.h.s.) LO term for L=2



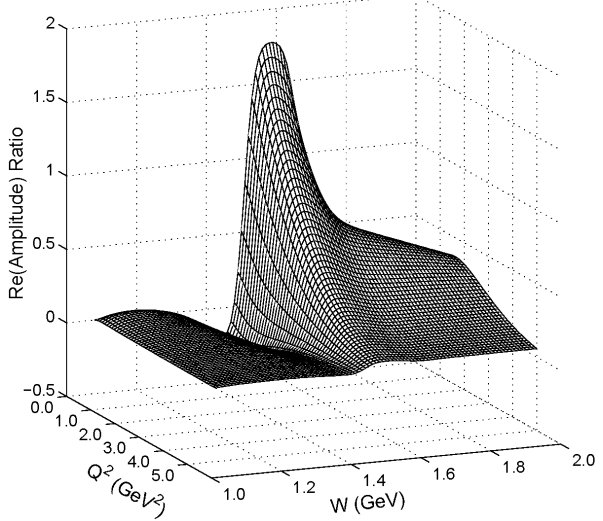
Re(r.h.s.) LO+NLO terms for L=2



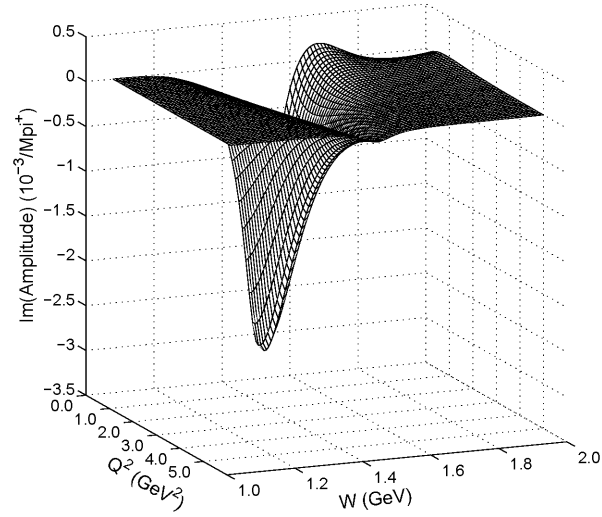
Amplitude ratio of Re LO terms for L=2



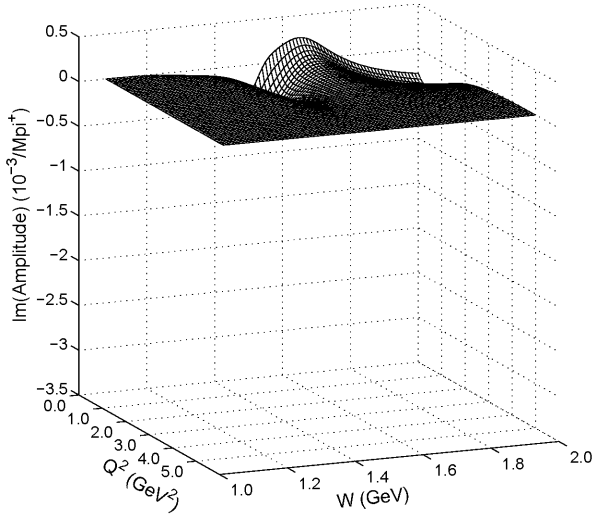
Amplitude ratio of Re LO+NLO terms for L=2



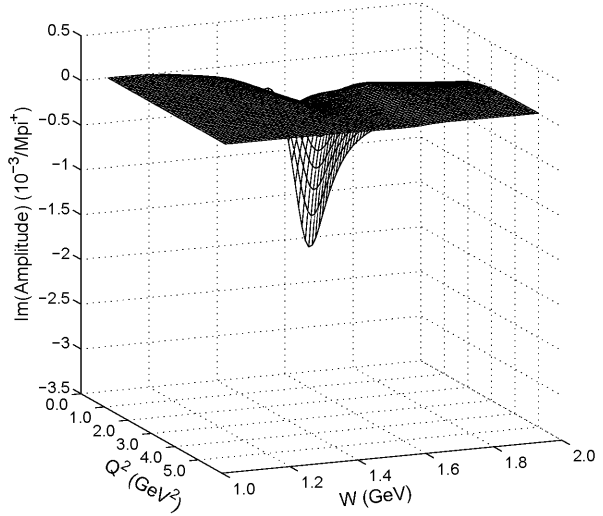
Im(l.h.s.) for L=2



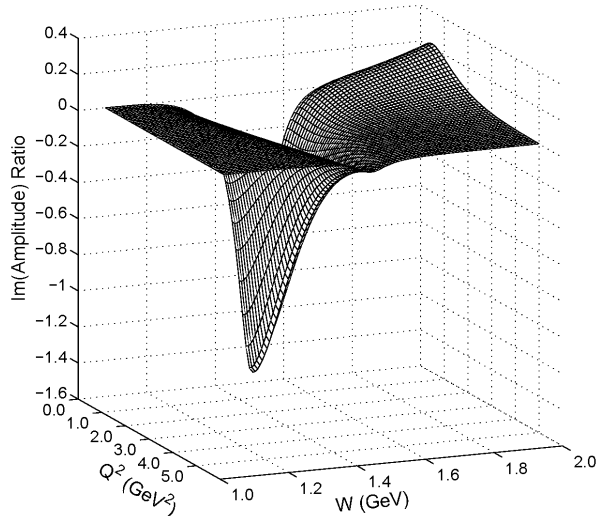
Im(r.h.s.) LO term for L=2



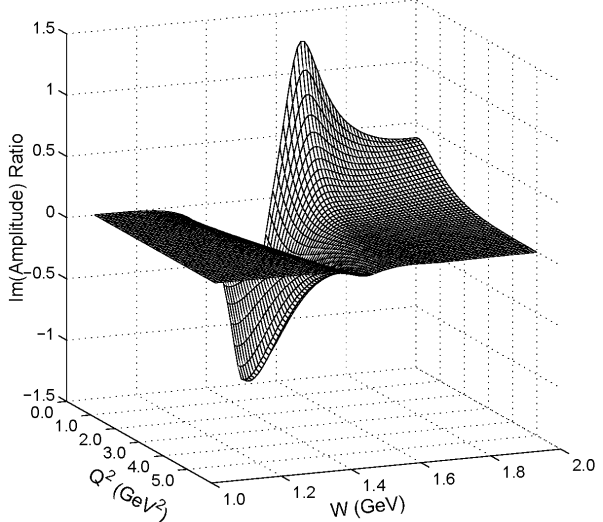
Im(r.h.s.) LO+NLO terms for L=2



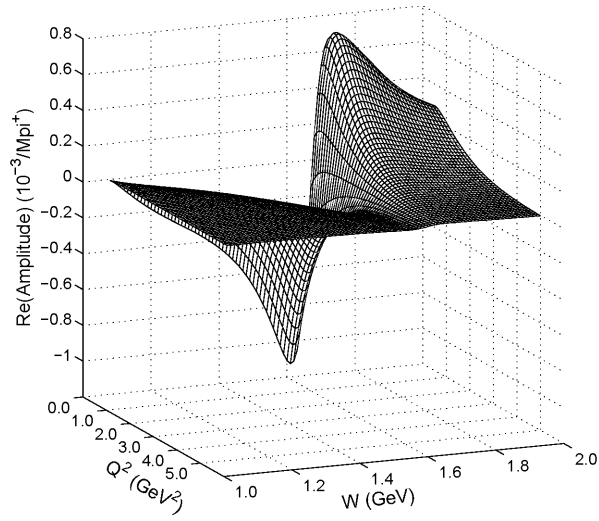
Amplitude ratio of Im LO terms for L=2



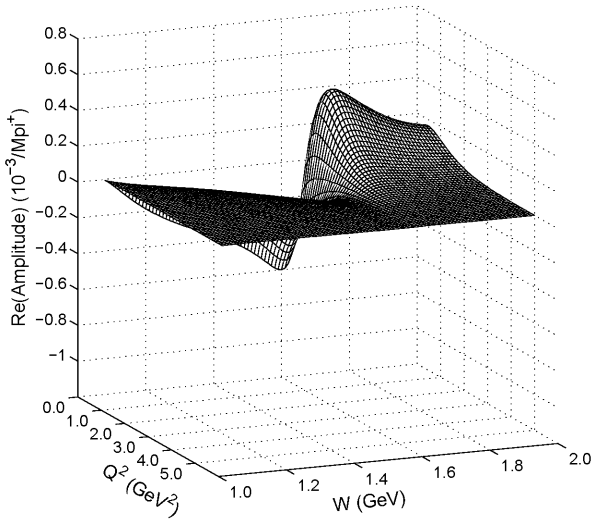
Amplitude ratio of Im LO+NLO terms for L=2



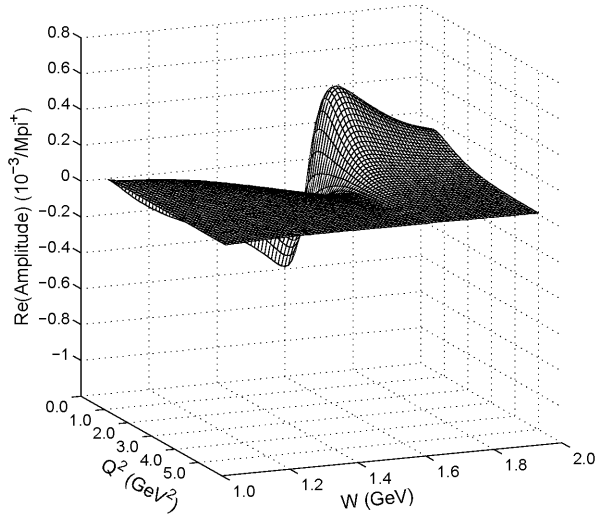
Re(l.h.s.) for L=3



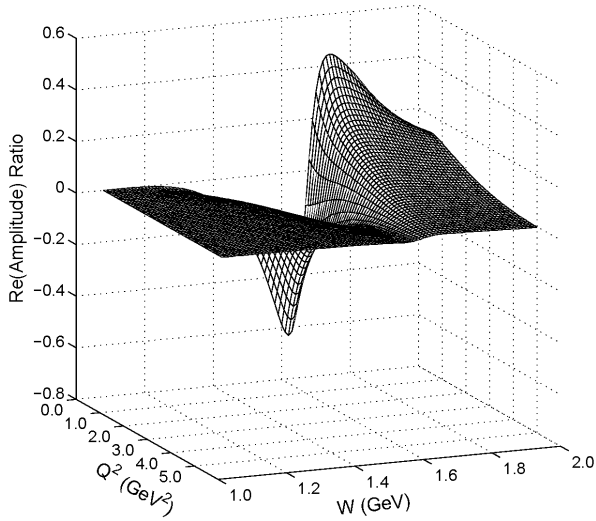
Re(r.h.s.) LO term for L=3



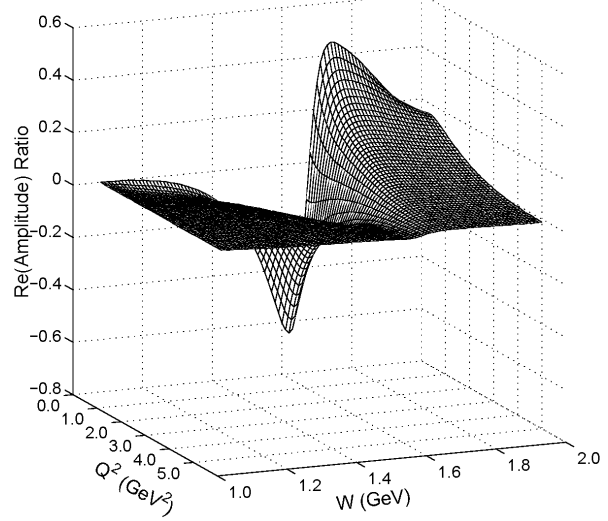
Re(r.h.s.) LO+NLO terms for L=3



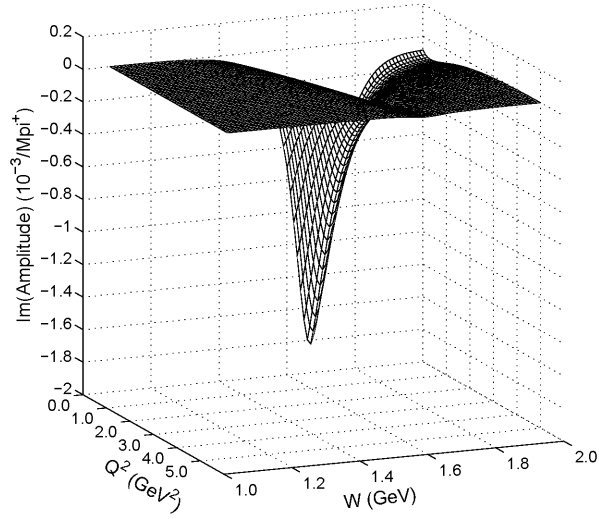
Amplitude ratio of Re LO terms for L=3



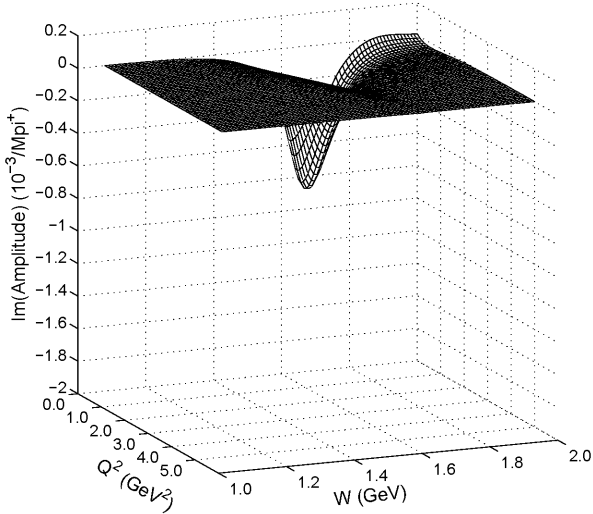
Amplitude ratio of Re LO+NLO terms for L=3



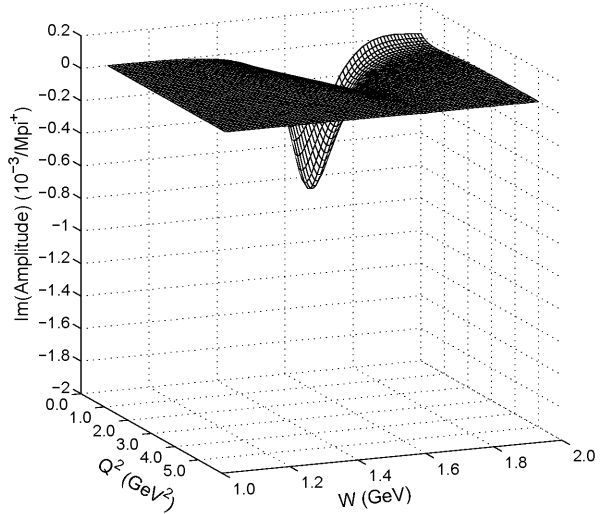
Im(l.h.s.) for L=3



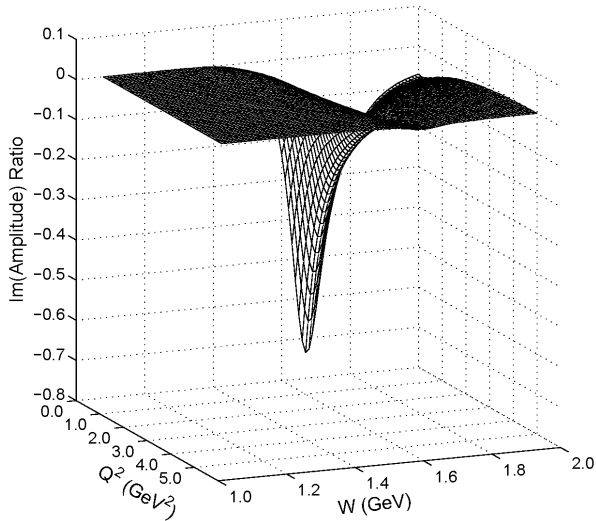
Im(r.h.s.) LO term for L=3



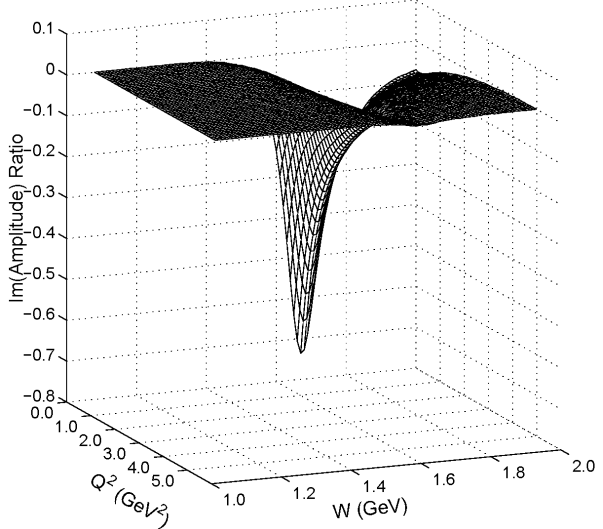
Im(r.h.s.) LO+NLO terms for L=3



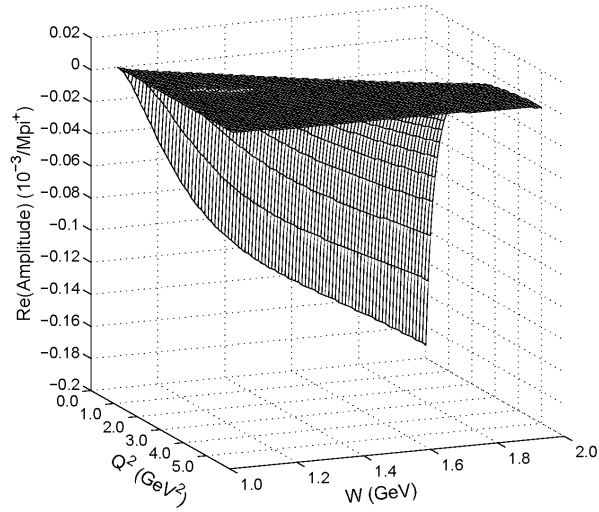
Amplitude ratio of Im LO terms for L=3



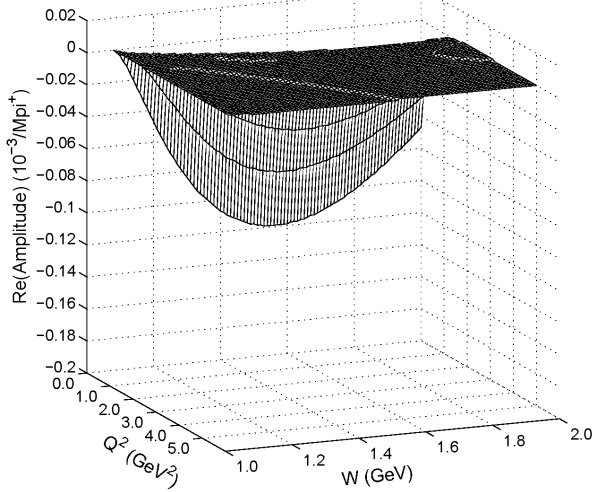
Amplitude ratio of Im LO+NLO terms for L=3



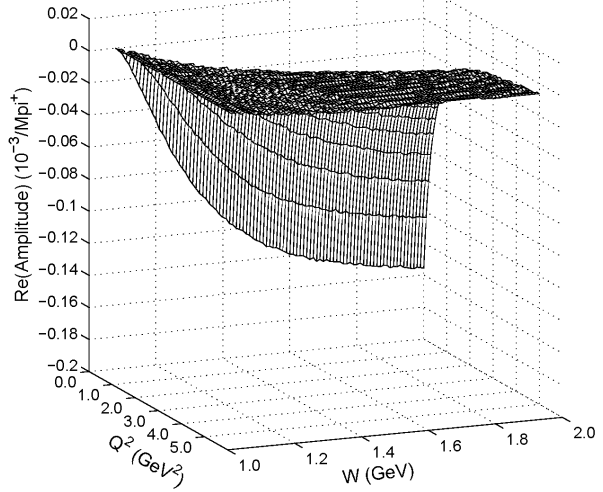
Re(l.h.s.) for L=4



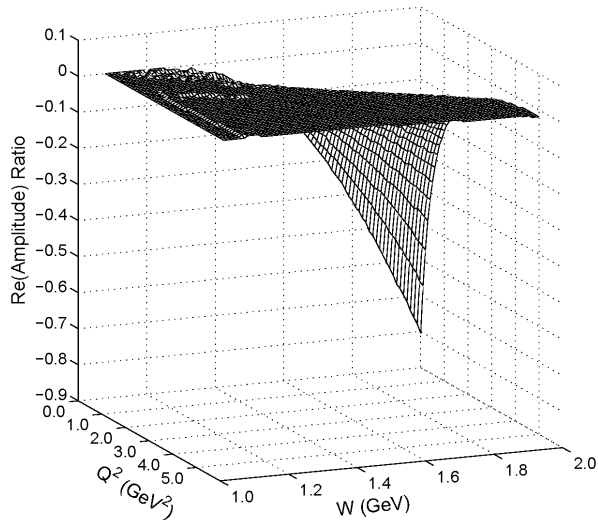
Re(r.h.s.) LO term for L=4



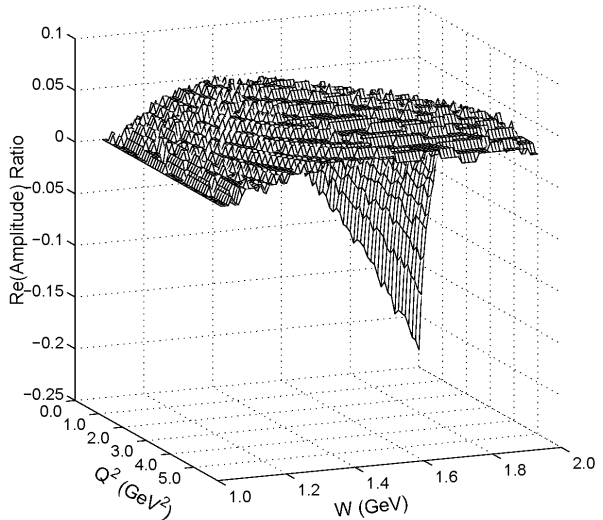
Re(r.h.s.) LO+NLO terms for L=4



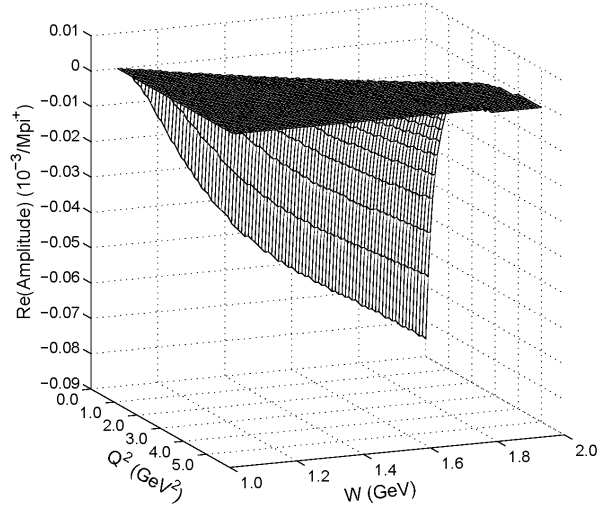
Amplitude ratio of Re LO terms for L=4



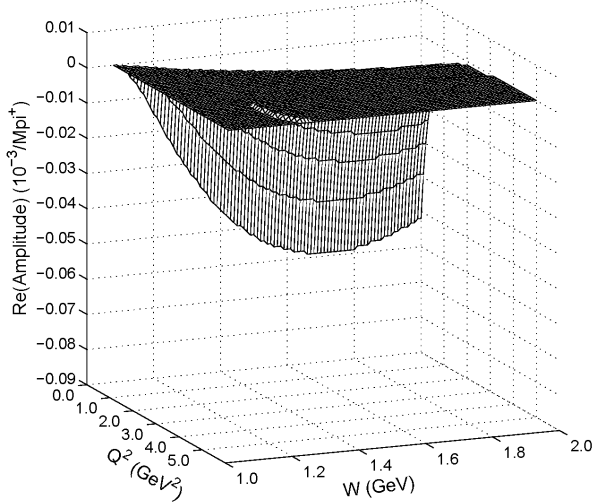
Amplitude ratio of Re LO+NLO terms for L=4



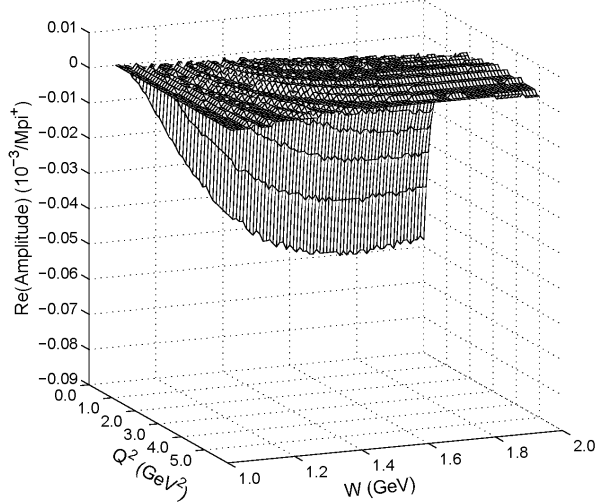
Re(l.h.s.) for L=5



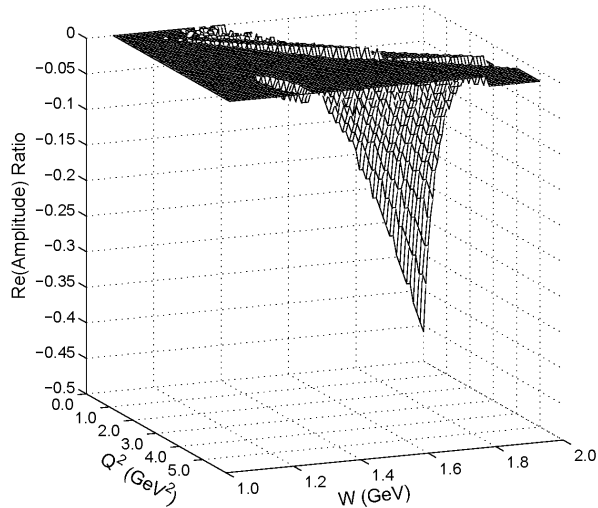
Re(r.h.s.) LO term for L=5



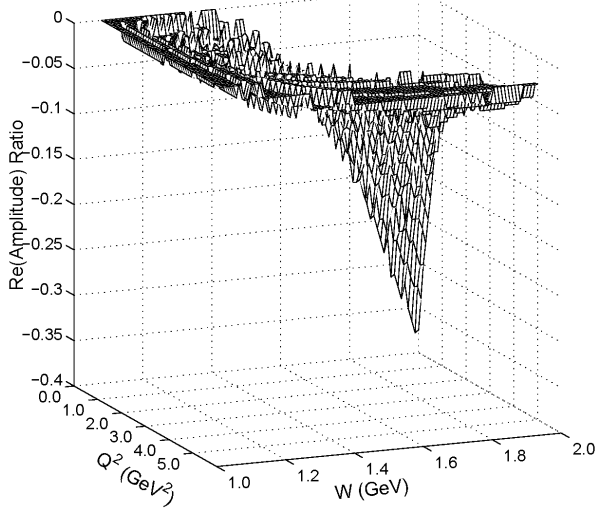
Re(r.h.s.) LO+NLO terms for L=5



Amplitude ratio of Re LO terms for L=5



Amplitude ratio of Re LO+NLO terms for L=5



- and D.R. Martin, Phys. Rev. D **70**, 016008 (2004) [arXiv:hep-ph/0404160]; N. Matagne and F. Stancu, Phys. Rev. D **71**, 014010 (2005) [arXiv:hep-ph/0409261]; Phys. Lett. B **631**, 7 (2005) [arXiv:hep-ph/0505118]; Phys. Rev. D **74**, 034014 (2006) [arXiv:hep-ph/0604122]; Nucl. Phys. A **811**, 291 (2008) [arXiv:hep-ph/0610099]; Phys. Rev. D **73**, 114025 (2006) [arXiv:hep-ph/0603032]; Phys. Rev. D **77**, 054026 (2008) [arXiv:0801.3575 [hep-ph]]; C. Semay, F. Buisseret, N. Matagne, and F. Stancu, Phys. Rev. D **75**, 096001 (2007) [arXiv:hep-ph/0702075].
- [4] G.S. Adkins, C.R. Nappi, and E. Witten, Nucl. Phys. B **228**, 552 (1983); G.S. Adkins and C.R. Nappi, Nucl. Phys. B **249**, 507 (1985).
- [5] T.H.R. Skyrme, Proc. Roy. Soc. Lond. A **260**, 127 (1961).
- [6] A. Hayashi, G. Eckart, G. Holzwarth, and H. Walliser, Phys. Lett. B **147**, 5 (1984); M.P. Mattis and M. Karliner, Phys. Rev. D **31**, 2833 (1985).
- [7] M.P. Mattis and M.E. Peskin, Phys. Rev. D **32**, 58 (1985); M.P. Mattis, Phys. Rev. Lett. **56**, 1103 (1986).
- [8] M.P. Mattis and M. Mukerjee, Phys. Rev. Lett. **61**, 1344 (1988).
- [9] J.L. Gervais and B. Sakita, Phys. Rev. Lett. **52**, 87 (1984); Phys. Rev. D **30**, 1795 (1984).
- [10] R.F. Dashen and A.V. Manohar, Phys. Lett. B **315**, 425 (1993) [arXiv:hep-ph/9307241]; **315**, 438 (1993) [arXiv:hep-ph/9307242].
- [11] R.F. Dashen, E.E. Jenkins, and A.V. Manohar, Phys. Rev. D **49**, 4713 (1994) [Erratum-ibid. D **51**, 2489 (1995)] [arXiv:hep-ph/9310379].
- [12] T.D. Cohen and R.F. Lebed, Phys. Rev. Lett. **91**, 012001 (2003) [arXiv:hep-ph/0301167]; Phys. Rev. D **67**, 096008 (2003) [arXiv:hep-ph/0301219]; Phys. Rev. D **68**, 056003 (2003) [arXiv:hep-ph/0306102].
- [13] T.D. Cohen, D.C. Dakin, A. Nellore, and R.F. Lebed, Phys. Rev. D **69**, 056001 (2004) [arXiv:hep-ph/0310120].
- [14] T.D. Cohen and R.F. Lebed, Phys. Lett. B **578**, 150 (2004) [arXiv:hep-ph/0309150].
- [15] T.D. Cohen and R.F. Lebed, Phys. Rev. D **70**, 096015 (2004) [arXiv:hep-ph/0408342]; Phys. Lett. B **619**, 115 (2005) [arXiv:hep-ph/0504200]; Phys. Rev. D **72**, 056001 (2005) [arXiv:hep-ph/0507267]; R.F. Lebed, Phys. Lett. B **639**, 68 (2006) [arXiv:hep-ph/0603150].
- [16] T.D. Cohen and R.F. Lebed, Phys. Rev. D **74**, 036001 (2006) [arXiv:hep-ph/0604175].
- [17] T.D. Cohen and R.F. Lebed, Phys. Rev. D **74**, 056006 (2006) [arXiv:hep-ph/0608038].

- [18] H.J. Kwee and R.F. Lebed, Phys. Rev. D **75**, 016002 (2007) [arXiv:hep-ph/0611035].
- [19] R.F. Dashen, E.E. Jenkins, and A.V. Manohar, Phys. Rev. D **51**, 3697 (1995) [arXiv:hep-ph/9411234].
- [20] D.B. Kaplan and M.J. Savage, Phys. Lett. B **365**, 244 (1996) [arXiv:hep-ph/9509371];
D.B. Kaplan and A.V. Manohar, Phys. Rev. C **56**, 76 (1997) [arXiv:nucl-th/9612021].
- [21] T.D. Cohen, D.C. Dakin, A. Nellore, and R.F. Lebed, Phys. Rev. D **70**, 056004 (2004) [arXiv:hep-ph/0403125].
- [22] H.J. Kwee and R.F. Lebed, JHEP **0710**, 046 (2007) [arXiv:hep-ph/0612267]; J. Phys. A **41**, 015206 (2008) [arXiv:0711.4340 [hep-ph]].
- [23] T.D. Cohen, D.C. Dakin, R.F. Lebed, and D.R. Martin, Phys. Rev. D **71**, 076010 (2005) [arXiv:hep-ph/0412294].
- [24] C.E. Carlson and C.D. Carone, Phys. Rev. D **58**, 053005 (1998) [arXiv:hep-ph/9804304];
N.N. Scoccola, J.L. Goity, and N. Matagne, Phys. Lett. B **663**, 222 (2008) [arXiv:0711.4203 [hep-ph]];
J.L. Goity and N.N. Scoccola, Phys. Rev. Lett. **99**, 062002 (2007) [arXiv:hep-ph/0701244].
- [25] D. Drechsel and L. Tiator, J. Phys. G **18**, 449 (1992).
- [26] D. Drechsel, S.S. Kamalov, and L. Tiator, Eur. Phys. J. A **34**, 69 (2007) [arXiv:0710.0306 [nucl-th]]; the MAID analysis is available at <http://www.kph.uni-mainz.de/maid/>.
- [27] V.B. Berestetskii, E.M. Lifshitz, and L.P. Pitaevskii, *Relativistic Quantum Theory*, (Addison-Wesley, Reading, MA, 1971).
- [28] A.R. Edmonds, *Angular Momentum in Quantum Mechanics* (Princeton Univ. Press, Princeton, NJ 1996).